

# Unified Modeling and Rate Coverage Analysis for Satellite-Terrestrial Integrated Networks: Coverage Extension or Data Offloading?

Jeonghun Park, Jinseok Choi, Namyoon Lee, and François Baccelli

## Abstract

With the growing interest in satellite networks, satellite-terrestrial integrated networks (STINs) have gained significant attention because of their potential benefits. However, due to the lack of a tractable network model for the STIN architecture, analytical studies allowing one to investigate the performance of such networks are not yet available. In this work, we propose a unified network model that jointly captures satellite and terrestrial networks into one analytical framework. Our key idea is based on Poisson point processes distributed on concentric spheres, assigning a random height to each point as a mark. This allows one to consider each point as a source of desired signal or a source of interference while ensuring visibility to the typical user. Thanks to this model, we derive the probability of coverage of STINs as a function of major system parameters, chiefly path-loss exponent, satellites and terrestrial base stations' height distributions and density, transmit power and biasing factors. Leveraging the analysis, we concretely explore two benefits that STINs provide: i) coverage extension in remote rural areas and ii) data offloading in dense urban areas.

## Index Terms

Satellite-terrestrial integrated network, stochastic geometry, rate coverage probability.

## I. INTRODUCTION

Recent advances in low Earth orbit (LEO) satellite technologies have brought breakthrough not only in the space industry, but also in wireless communications. With the decreasing cost of

J. Park is with School of Electrical and Electronic Engineering, Yonsei University, South Korea (e-mail: jhpark@yonsei.ac.kr). J. Choi is with School of Electrical Engineering, KAIST, South Korea (email: jinseok@kaist.ac.kr), N. Lee is with Department of Electrical Engineering, Korea University, South Korea (e-mail: namyoon@korea.ac.kr). F. Baccelli is with INRIA-ENS, France (email: francois.baccelli@ens.fr)

launching LEO satellites, tens of thousands of LEO satellites are planned to be deployed (e.g., SpaceX Starlink [1]), which enables the structuration of ultra-dense wireless networks above the Earth. One promising way to leverage satellite networks is to integrate them with the existing terrestrial network, creating a mutually complementary system that operates seamlessly [2]–[4]. This motivates the advent of satellite-terrestrial integrated networks (STINs). In the literature, two main benefits of STINs have mainly been discussed:

- **Coverage extension:** Unlike terrestrial base stations (BSs) whose deployment can be limited in remote areas, satellites provide a relatively uniform density across all locations. For this reason, the coverage region can be extended thanks to STINs [2], [4].
- **Data offloading:** In high traffic cases, pushing data traffic to the satellite network improves the rate coverage performance by balancing the loads [5]–[7].

Notwithstanding these potential advantages, there has been a dearth of analytical studies investigating the rate coverage performance of STINs. A main hindrance is the lack of a unified network model that jointly captures satellite and terrestrial networks simultaneously. In this work, we address this challenge by proposing such a unified model. Leveraging this model, we analyze the rate coverage performance of STINs, which allows one to foresee the benefits of these new architectures.

#### *A. Related Work*

The use of stochastic geometry has played a crucial role in modeling and analyzing wireless networks [8], [9]. In particular, much of the prior work has focused on the investigation of terrestrial cellular networks. This analysis involves the distribution of a random point process on the 2D plane to model the spatial locations of the BSs. With this methodology, a wide range of cellular network types, including HetNets [10], [11], multi-antenna cellular networks [12], [13], millimeter wave (mmWave) cellular networks [14], [15], and UAVs networks [16], [17] were actively explored.

Recently, with the growing interest in satellite communication systems, satellite network analysis based on tools of stochastic geometry gained great momentum [18]–[24]. For instance, in [20], the coverage probability of satellite networks was derived by modeling the satellite locations as a binomial point process (BPP) distributed on a certain sphere. This work was improved in [21] by incorporating a non-homogeneous distribution of satellites. In [22], the technique of [20] was employed with different fading scenarios. Despite the popularity of the BPP based analysis,

this model inevitably entails complicated expressions, which limits tractability. Addressing this, in [24], an analytical approach exploiting conditional Poisson point process (PPP) was proposed, wherein the PPP was distributed on a certain sphere. The coverage analysis was then conducted by conditioning on the fact that at least 1 satellite is visible to the typical user. This makes the analytical expressions much more tractable than those of the BPP. Additionally, it was also shown that the analysis of [24] reflects well the actual coverage trend drawn by using realistic Starlink constellation sets.

Compared to the analysis of terrestrial networks, one crucial difference in the modeling of satellite networks is the use of a spherical point process, wherein a random point process (either PPP or BPP) is distributed on a certain sphere to model the satellite locations. The disparity between the modeling methodology used for the satellite and terrestrial networks (i.e., a planar point process vs. a spherical point process) is the main challenge to unify them into a single model for analyzing the STIN. There exists a few works on the analysis of the cooperation between non-terrestrial and terrestrial networks [25], [26]. However, their models are oversimplified. For example, [26] considered a spherical point process for modeling satellite networks and a planar point process for modeling terrestrial networks separately, which cannot capture the full geometries of STINs. In [25], a single satellite was considered, which is not adequate when dealing with dense satellite networks. Consequently, there is a gap in the literature regarding the rate coverage analysis of the STIN with a unified network modeling, and this gap is the primary motivation of our work.

### *B. Contributions*

In this paper, we consider the downlink of a STIN, in which a user can be served either from a satellite or a terrestrial BS sharing the same spectrum (i.e., the scenario is referred as an open network). The user selects its association based on the averaged reference signal power including bias factors, where the latter can be used to control the load as in heterogeneous networks (HetNets) [10], [11]. Further, the user experiences the interference coming from both the satellites and the terrestrial BSs. In this setup, our aim is to model and analyze the rate coverage performance of the considered STIN, and to provide STIN system design insights leveraging the analysis. We summarize our contributions as follows.

- **Unified modeling:** For modeling the STIN, it is of central importance to jointly capture the key characteristics of the satellite and the terrestrial networks. Since this is not feasible

with the existing network models, we propose a novel network model. In our model, a homogeneous PPP is first distributed on two concentric spheres, where the inner sphere represents the Earth and the outer sphere represents the satellite orbital sphere. Then, a random height is assigned to each point, so that each satellite and terrestrial BS has a different altitude. This is a key distinguishable point from the previous models [18]–[20], [24] where all points are at the same altitude. The random height feature has two important motivations. First, this makes our model more realistic, as it can reflect a realistic satellite network where satellites have different altitudes [1]. Second, the random height is a key to unify the satellite and the terrestrial networks into a single analytical framework. Without positive random height, the terrestrial network cannot be modeled by using a spherical point process distributed on the Earth since there is no mathematical visibility between a user and any other terrestrial BS. We will explain this in more detail in Remark 1.

- **Rate coverage analysis:** Based on the proposed model, we derive an expression for the coverage probability as a function of the system parameters, chiefly the densities, path-loss exponents, height geometries (maximum/minimum altitudes and height distributions), and bias factors of the satellites and the terrestrial BSs. To this end, we first obtain the visibility probability of the satellite and the terrestrial networks, that characterizes the probability that a user sees at least 1 satellite/terrestrial BS that it can communicate with. We note that this is not straightforward from the existing result [24] since each satellite/terrestrial BS has a random altitude in our model. Using this, we compute the conditional nearest satellite/terrestrial BS distance distribution and also the probability that a user is associated with the satellite/terrestrial network. Leveraging these, we derive the rate coverage probability of the STIN under the Nakagami- $m$  fading assumption and discuss upper/lower bounds on the rate coverage.
- **Analysis of STIN benefits and design insights:** Using our analysis, we concretely explore the two benefits of the STIN architecture: coverage extension in remote rural areas and data offloading in dense urban areas. This leads to some valuable system design insights: 1) In remote rural areas where the terrestrial BSs' deployment density is very low, the STIN offers huge coverage enhancement. However, due to satellite interference, it is crucial to control the satellite density properly. 2) In dense urban areas where the user density is high, in the STIN, data traffic can be pushed to the satellite from the terrestrial BSs, provided that satellite density and the bias are suitably selected.

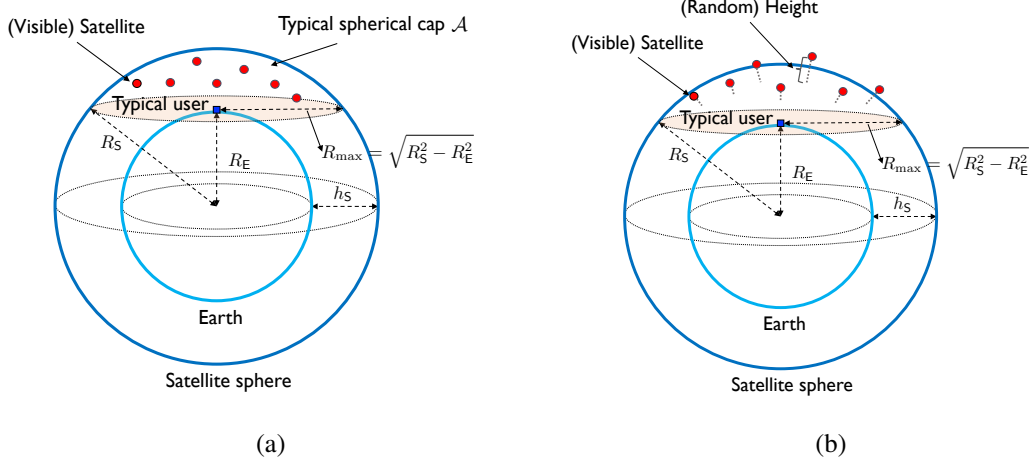


Fig. 1: An illustration to compare (a) the conventional satellite network model and (b) the proposed satellite network with random heights. As seen in the figure, the proposed network model includes the conventional model as a special case where all the heights of the satellites are the same.

The remaining part of the paper is structured as follows. In Section II, we present the system model used through this paper, including our unified modeling for the STIN. In Section III, we derive key mathematical lemmas required to obtain the rate coverage probability, which is computed in Section IV. In Section V, we investigate the benefits of the STIN. Section VI concludes the paper.

## II. SYSTEM MODEL

### A. Network Model

**Poisson point process on a sphere:** To model the spatial locations of satellite and terrestrial BS, we consider PPPs distributed on a sphere (SPPP) [24]. For better understanding, we first introduce a generic SPPP model with random heights, and then present the specific model for the satellite and terrestrial networks, respectively.

Consider a sphere defined in  $\mathbb{R}^3$  whose center is the origin  $\mathbf{0}$  and radius is fixed as  $R$ . This sphere is denoted as  $\mathbb{S}_R^2 = \{\mathbf{x} \in \mathbb{R}^3 : \|\mathbf{x}\|_2 = R\}$ . Let  $\Phi$  be an isotropic PPP on  $\mathbb{S}_R^2$ . We denote the point of this point process as  $\{\mathbf{d}_i, 1 \leq i \leq N, \|\mathbf{d}_i\|_2 = R\}$  and denote the density of  $\Phi$  as  $\lambda$ . The number of points on the sphere  $N$  is a random variable drawn from the Poisson distribution with mean  $\lambda|\mathbb{S}_R^2| = 4\pi R^2\lambda$ . Conditional on the fact that there are  $k$  points, these

points are independently and uniformly distributed on  $\mathbb{S}_R^2$ . The number of points of  $\Phi$  located in a particular set  $\mathcal{A} \subset \mathbb{S}_R^2$  is denoted as  $\Phi(\mathcal{A})$ .

**Random heights:** Based on the PPP  $\Phi$ , we construct a new point process by displacing each point of  $\Phi$  from the sphere by a certain height. Denoting  $h_{\mathbf{d}_i}$  by the height of point  $\mathbf{d}_i$ , we define the new point as  $\hat{\mathbf{d}}_i = \mathbf{d}_i \cdot (R + h_{\mathbf{d}_i})/R$ , so that  $\|\hat{\mathbf{d}}_i\| = R + h_{\mathbf{d}_i}$ . The heights of the points are assume to be independent and identically distributed (IID) random variables drawn from a certain distribution  $f_H$  on  $\mathbb{R}^+$ . Correspondingly, we let  $F_H$  be the cumulative distribution function (CDF) of the heights. The points of this point process are hence  $\hat{\Phi} = \{\hat{\mathbf{d}}_i, 1 \leq i \leq N, \|\hat{\mathbf{d}}_i\|_2 = R + h_{\mathbf{d}_i}, h_{\mathbf{d}_i} \sim f_H\}$ . Note that  $\hat{\Phi}$  can be seen as a marked PPP generated from  $\Phi$ , wherein the mark of the point on  $\mathbf{d}_i$  is the height  $h_{\mathbf{d}_i}$ . Throughout the paper, we assume a positive height,  $h_{\mathbf{d}_i} \geq 0, \forall \mathbf{d}_i \in \Phi$ .

**Satellite network:** We now describe the satellite network model. Consider two spheres sharing the same origin. We define the radii of these spheres as  $R_E$  and  $R_S$ , respectively. The sphere with radius  $R_E$  represents the Earth and the sphere with radius  $R_S$  represents the satellite orbital sphere. We also define  $h_S = R_S - R_E$ , where  $h_S$  is the standard satellite altitude. We now distribute a SPPP on  $\mathbb{S}_{R_S}^2$ , denoted as  $\Phi_S = \{\mathbf{d}_i^S, 1 \leq i \leq N_S, \|\mathbf{d}_i^S\|^2 = R_S\}$  with density  $\lambda_S$ . Upon this, we displace point  $\mathbf{d}_i^S$  from the satellite orbital sphere by a random height  $h_{\mathbf{d}_i^S}$ , which builds  $\hat{\Phi}_S = \{\hat{\mathbf{d}}_i^S, 1 \leq i \leq N_S, \|\hat{\mathbf{d}}_i^S\|^2 = R_S + h_{\mathbf{d}_i^S}, h_{\mathbf{d}_i^S} \sim f_{H_S}\}$ . The support of  $f_{H_S}$  will be denoted as  $\mathcal{H}_S$ . In this modeling,  $\hat{\Phi}_S$  represents a snapshot of the satellite spatial locations. If  $h_{\mathbf{d}_i^S} = 0$  for all  $i$ , then each satellite is located at the same altitude of  $h_S$ , which corresponds to the network model in [24].

We depict the conventional satellite network model without random heights and the considered satellite network model with random heights in Fig 1.

**Terrestrial network:** Similar to the satellite network, we consider a SPPP with random heights to model the terrestrial network. We first distribute a SPPP with the density  $\lambda_T$  on the sphere with radius  $R_E$  and denote this point process as  $\Phi_T$ . Subsequently, incorporating random heights  $h_{\mathbf{d}_i^T} \sim f_{H_T}$  into  $\Phi_T$ , we have  $\hat{\Phi}_T = \{\hat{\mathbf{d}}_i^T, 1 \leq i \leq N_T, \|\hat{\mathbf{d}}_i^T\|^2 = R_T + h_{\mathbf{d}_i^T}, h_{\mathbf{d}_i^T} \sim f_{H_T}\}$ . A snapshot of the spatial locations of terrestrial BSs is modeled by  $\hat{\Phi}_T$ . The support of  $f_{H_T}$  is denoted by  $\mathcal{H}_T$ . If  $h_{\mathbf{d}_i^T} = 0$  for all  $i$ , all terrestrial BSs are located on the surface of the Earth. We also assume  $h_{\mathbf{d}_i^T} \geq 0$ .

**Typical user:** We also model the users' locations as a homogeneous SPPP  $\Phi_U = \{\mathbf{u}_i, 1 \leq i \leq N_U, \|\mathbf{u}_i\|_2 = R_E\}$  with density  $\lambda_U$ . Per Slivnyak's theorem [8], we focus on the typical

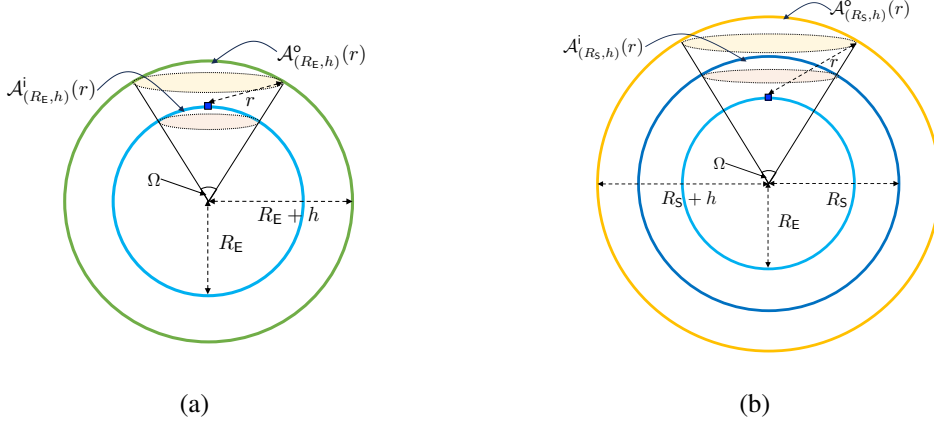


Fig. 2: An illustration to explain the outer/inner typical spherical cap: (a) the outer/inner typical spherical caps in the terrestrial network and (b) the outer/inner typical spherical caps in the satellite network.

user  $\mathbf{u}_1$  located on  $(0, 0, R_E)$  in Cartesian coordinates. We point out that this does not affect the statistical distribution of  $\hat{\Phi}_S$  and  $\hat{\Phi}_T$ . Note that the considered user model corresponds to a uniform traffic demand scenario. More realistic traffic demands, e.g., a heavy traffic demand in an urban environments and a light traffic demand in a rural areas will be discussed later.

**Typical spherical cap:** Since the satellites and the terrestrial BSs are distributed on certain spheres, some points are not visible from the typical user. If so, they are neither counted as a potential source of desired signal nor as contributing to the interference. For this reason, characterizing the visibility is crucial in the coverage analysis. To this end, we use the concept of typical spherical cap.

At first, we focus on the terrestrial network. Consider a point  $\mathbf{d} \in \Phi_T$  is on sphere  $\mathbb{S}_{R_E}^2$  and its image point  $\hat{\mathbf{d}} \in \hat{\Phi}_T$  with height  $h$ , so that  $\hat{\mathbf{d}}$  is on sphere  $\mathbb{S}_{R_E+h}^2$ . Recalling that the typical user is located at  $(0, 0, R_E)$ , the *outer* typical spherical cap of radius  $r$ ,  $\mathcal{A}_{(R_E, h)}^o(r)$ , is defined as the set of points in  $\mathbb{S}_{R_E+h}^2$  whose distance to the typical user is no larger than  $r$ :

$$\mathcal{A}_{(R_E, h)}^o(r) = \{ \mathbf{z} \in \mathbb{S}_{R_E+h}^2 : \|\mathbf{z} - \mathbf{u}_1\|_2 \leq r \}. \quad (1)$$

We provide an illustration for  $\mathcal{A}_{(R_E, h)}^o(r)$  in Fig. 2-(a). It is worth to mention that given  $h$ , we will focus on  $r_{\min} \leq r \leq r_{\max}$ , with

$$r_{\min} = h, \quad r_{\max} = \sqrt{h(h + 2R_E)}. \quad (2)$$

If  $r = r_{\max}$ , then  $\mathcal{A}_{(R_E, h)}^{\circ}(r_{\max})$  is the portion of sphere  $\mathbb{S}_{R_E+h}^2$  cut off by the plane tangent to the sphere  $\mathbb{S}_{R_E}^2$  (the Earth) at  $(0, 0, R_E)$ . The *inner* typical spherical cap  $\mathcal{A}_{(R_E, h)}^i(r)$  is the spherical cap of  $\mathbb{S}_{R_E}^2$  that has the same solid angle as  $\mathcal{A}_{(R_E, h)}^{\circ}(r)$ , namely,

$$\mathcal{A}_{(R_E, h)}^i(r) = \left\{ \mathbf{z} \in \mathbb{S}_{R_E}^2 : \left\| \frac{R_E + h}{R_E} \cdot \mathbf{z} - \mathbf{u}_1 \right\|_2 \leq r \right\}. \quad (3)$$

We also provide an illustration of the inner typical spherical cap  $\mathcal{A}_{(R_E, h)}^i(r)$  in Fig. 2-(a). In Fig. 2, we observe that, seen from the origin, the solid angles  $\Omega$  of  $\mathcal{A}_{(R_E, h)}^{\circ}(r)$  and  $\mathcal{A}_{(R_E, h)}^i(r)$  are the same. The inner typical spherical cap  $\mathcal{A}_{(R_E, h)}^i(r)$  is the region of the points  $\mathbf{d} \in \Phi_{\tau}$  which are mapped to the points  $\hat{\mathbf{d}} \in \mathcal{A}_{(R_E, h)}^{\circ}(r)$ .

Now we investigate the areas of the typical spherical caps. In the terrestrial network, the area of the outer typical spherical cap  $\mathcal{A}_{(R_E, h)}^{\circ}(r)$  is obtained as

$$|\mathcal{A}_{(R_E, h)}^{\circ}(r)| = 2\pi(h - h_r)(R_E + h), \quad (4)$$

where

$$h_r = \frac{(R_E + h)^2 - R_E^2 - r^2}{2R_E}, \quad (5)$$

by using Archimedes' Hat-Box Theorem [27]. By the definition of the solid angle, we have

$$\Omega = \frac{|\mathcal{A}_{(R_E, h)}^{\circ}(r)|}{(R_E + h)^2} = \frac{2\pi \left( h - \frac{(R_E + h)^2 - R_E^2 - r^2}{2R_E} \right)}{R_E + h}. \quad (6)$$

Then the area of the inner typical spherical cap  $\mathcal{A}_{(R_E, h)}^i(r)$  is given by

$$|\mathcal{A}_{(R_E, h)}^i(r)| = \Omega R_E^2 = \frac{2\pi R_E^2 \left( h - \frac{(R_E + h)^2 - R_E^2 - r^2}{2R_E} \right)}{R_E + h}. \quad (7)$$

When  $r = r_{\max}$ , the area of the outer/inner typical spherical caps are simplified to

$$|\mathcal{A}_{(R_E, h)}^{\circ}(r_{\max})| = 2\pi h(R_E + h), \quad |\mathcal{A}_{(R_E, h)}^i(r_{\max})| = \frac{2\pi h}{R_E + h} R_E^2. \quad (8)$$

When  $r = r_{\min}$ , the areas of the outer/inner typical spherical caps are 0.

Next, similar to the terrestrial network case, we define the outer and the inner typical spherical caps corresponding to the satellite network as  $\mathcal{A}_{(R_S, h)}^{\circ}(r)$  and  $\mathcal{A}_{(R_S, h)}^i(r)$  by following (1) and (3). Specifically, we have

$$\mathcal{A}_{(R_S, h)}^{\circ}(r) = \left\{ \mathbf{z} \in \mathbb{S}_{R_S+h}^2 : \|\mathbf{z} - \mathbf{u}_1\|_2 \leq r \right\}, \quad (9)$$

where  $r_{\min} \leq r \leq r_{\max}$  with

$$r_{\min} = R_S + h - R_E, \quad r_{\max} = \sqrt{(R_S + h)^2 - R_E^2}. \quad (10)$$



The area of the outer typical spherical cap is calculated as

$$|\mathcal{A}_{(R_S, h)}^o(r)| = 2\pi(h_S + h - h_r)(R_S + h), \quad h_r = \frac{(R_S + h)^2 - R_E^2 - r^2}{2R_E}. \quad (11)$$

Accordingly, when  $r = r_{\max}$ , then

$$|\mathcal{A}_{(R_S, h)}^o(r_{\max})| = 2\pi(h_S + h)(R_S + h). \quad (12)$$

The inner typical spherical cap is defined as

$$\mathcal{A}_{(R_S, h)}^i(r) = \left\{ \mathbf{z} \in \mathbb{S}_{R_S}^2 : \left\| \frac{R_S + h}{R_S} \cdot \mathbf{z} - \mathbf{u}_1 \right\|_2 \leq r \right\}, \quad (13)$$

where its area is

$$|\mathcal{A}_{(R_S, h)}^i(r)| = \Omega R_S^2 = \frac{2\pi R_S^2 \left( h_S + h - \frac{(R_S + h)^2 - R_E^2 - r^2}{2R_E} \right)}{R_S + h}. \quad (14)$$

When  $r = r_{\min}$ , the areas of the outer/inner typical spherical caps are 0. We depict the outer/inner typical spherical caps of the satellite network in Fig. 2-(b).

With the defined typical spherical caps, we are able to identify the visibility of the terrestrial BSs or the satellites. For example, in the terrestrial network, the terrestrial BS with height  $h$  (located at  $\hat{\mathbf{d}}_i^\top$ ) is visible to the typical user if and only if  $\hat{\mathbf{d}}_i^\top \in \mathcal{A}_{(R_E, h)}^o(r_{\max})$  (or equivalently,  $\mathbf{d}_i^\top \in \mathcal{A}_{(R_E, h)}^i(r_{\max})$ ). This is because, if  $\hat{\mathbf{d}}_i^\top \notin \mathcal{A}_{(R_E, h)}^o(r_{\max})$ , then  $\hat{\mathbf{d}}_i^\top$  is located below the horizon, and the visibility is blocked by the Earth. The satellite visibility is also identified in an equivalent manner.

To characterize the visibility, we assume a set of terrestrial BSs whose heights are in  $[h, h + \Delta h]$  and denote such a point process as  $\hat{\Phi}_T^h \subset \hat{\Phi}_T$  and  $\Phi_T^h \subset \Phi_T$ . The event that the typical user can observe at least 1 terrestrial BS is equivalent with the event that any of  $\Phi_T^h$  includes at least 1 visible terrestrial BS, namely,

$$\mathcal{V}_T = \bigcup_{h \in \mathcal{H}_T} \{ \Phi_T^h(\mathcal{A}_{(R_E, h)}^i(r_{\max})) \geq 1 \}. \quad (15)$$

Similar to this, denoting a point process of the satellites with heights included in  $[h, h + \Delta h]$  as  $\hat{\Phi}_S^h \subset \hat{\Phi}_S$  and  $\Phi_S^h \subset \Phi_S$ , the event that the typical user can observe at least 1 satellite is

$$\mathcal{V}_S = \bigcup_{h \in \mathcal{H}_S} \{ \Phi_S^h(\mathcal{A}_{(R_S, h)}^i(r_{\max})) \geq 1 \}. \quad (16)$$

For simplicity, we denote the average number of visible satellites and of visible terrestrial BSs as  $\bar{N}_S$  and  $\bar{N}_T$ , respectively.

One key difference of the visibility in the proposed network model and the conventional network model [24] is that, in the proposed network model, the visibility is jointly determined not only by the points' spatial locations, but also their heights. Namely, even if two satellites are located at the same position in  $\Phi_S$ , it is possible that one satellite is visible and the other one is not because of their different altitudes. In general, the higher the altitude, the more likely the visibility of the point from the typical user. This is the main reason to define multiple typical spherical caps depending on  $h$ .

### B. Channel Model

The path-loss between the satellite located at  $\hat{\mathbf{d}}_i^S$  and the typical user located at  $\mathbf{u}_1$  is defined as  $\|\hat{\mathbf{d}}_i^S - \mathbf{u}_1\|^{-\beta_S}$ , where  $\beta_S$  is the path-loss exponent for the satellite network. Likewise, the path-loss between the terrestrial BS located at  $\hat{\mathbf{d}}_i^T$  and the typical user is defined as  $\|\hat{\mathbf{d}}_i^T - \mathbf{u}_1\|^{-\beta_T}$ , where  $\beta_T$  is the path-loss exponent for the terrestrial network. The wireless propagation environments of the satellite network and the terrestrial network are reflected into  $\beta_S$  and  $\beta_T$ . For instance, if the propagation between a satellite and a user is line-of-sight (LoS), then  $\beta_S = 2$ . If we consider an urban communication scenario with rich scattering for the terrestrial network,  $\beta_T = 4$ .

As the small-scale fading model, we use the Nakagami- $m$  distribution as it is capable of incorporating various fading scenarios such as the Rayleigh fading or the Rician fading. In this model,  $\sqrt{X_i^S}$ , which is the fading coefficient between satellite  $\hat{\mathbf{d}}_i^S$  and the typical user, is distributed according to the probability density function (PDF) given by [28]:

$$f_{\sqrt{X_i^S}}(x) = \frac{2m_S^{m_S}}{\Gamma(m_S)} x^{2m_S-1} \exp(-m_S x^2), \quad (17)$$

where  $x \geq 0$  and  $\Gamma(\cdot)$  is the Gamma function. We note that the satellite network scenario can be reduced to the Rayleigh fading ( $m_S = 1$ ) or the Rician- $K$  fading ( $m_S = \frac{(K+1)^2}{2K+1}$ ) by tuning  $m_S$ . Similar to this, in the terrestrial network,  $\sqrt{X_i^T}$ , which is the fading coefficient between terrestrial BS  $\hat{\mathbf{d}}_i^T$  and the typical user, also follows the Nakagami- $m$  distribution with parameter  $m_T$ .

We now explain the directional beamforming gain model. We adopt the sectorized antenna model, wherein the directional beamforming gains are approximated as a rectangular function [14], [29]. In such an approximation, a user gets the main-lobe gain when it is included within the main-lobe, otherwise the user has the side-lobe gain. The sectorized antenna model has been widely used in stochastic geometry based analysis because it is not only analytically tractable,

but it is also suitable to reflect the primary features of the directional beamforming. In this model, the beamforming gains in the satellite network are expressed as

$$G_S = G_S^{\text{tx}} G^{\text{rx}} \frac{c^2}{(4\pi f_c)^2}, \quad \bar{G}_S = \bar{G}_S^{\text{tx}} \bar{G}^{\text{rx}} \frac{c^2}{(4\pi f_c)^2}, \quad (18)$$

where  $G_S^{\text{tx}}$  (or  $\bar{G}_S^{\text{tx}}$ ) is the main-lobe (or the side-lobe) beamforming gains offered at a satellite, and  $G^{\text{rx}}$  (or  $\bar{G}^{\text{rx}}$ ) is the main-lobe (or the side-lobe) beamforming gains obtained at a user. We assume that only the associated satellite has  $G_S$  and the other interfering satellites have  $\bar{G}_S$ . The beamforming gains in the terrestrial network are defined in the similar manner. Namely, the associated terrestrial BS has the beamforming gain  $G_T$  and the other terrestrial BS has the beamforming gain  $\bar{G}_T$ .

### C. Cell Association

To control the user populations connected to each network, we apply the biasing factors in association process. When the satellites and the terrestrial BSs use different transmit power ( $P_S$  and  $P_T$ ) and biasing factors ( $B_S$  and  $B_T$ ), each satellite and terrestrial BS sends reference signals by encompassing the biasing factors, so that the effective transmit power of the reference signal is  $P_S B_S$  or  $P_T B_T$ . Averaging the randomness regarding the small-scale fading, the typical user is associated with a cell (either in the satellite or the terrestrial networks) whose average received power is strongest. Namely, the associated network  $o^*$  and the associated cell index  $k^*$  are determined by

$$(o^*, k^*) = \arg \max_{o \in \{T, S\}, k \in \mathbb{N}} P_o B_o \|\hat{\mathbf{d}}_k^o - \mathbf{u}_1\|^{-\beta_o}. \quad (19)$$

Throughout the paper, we use  $o^*$  to indicate the network type that the typical user is associated with and assume  $k^* = 1$  without loss of generality. The cell association is entangled with visibility. For instance, if there is no visible satellite, then we cannot have  $\{o^* = S\}$ . For this reason,  $(o^* = S)$  (or  $(o^* = T)$ ) implicitly means that there exists at least 1 satellite (or terrestrial BS) visible to the typical user.

### D. Performance Metric

We separately consider the association cases: 1) association with the satellite network ( $o^* = S$ ), 2) association with the terrestrial network ( $o^* = T$ ). At first, under the assumption that the typical user is associated with the satellite network, the conditional SINR is defined as

$$\text{SINR}_{|S} = \frac{G_S P_S X_1^S \|\hat{\mathbf{d}}_1^S - \mathbf{u}_1\|^{-\beta_S}}{I_{S|S} + I_{T|S} + \sigma^2}. \quad (20)$$

In (20),  $\sigma^2$  is the noise power and  $I_{S|S} = \sum_{\mathbf{d}_i^S \in \tilde{\mathcal{B}}_{S|S}} \bar{G}_S P_S X_i^S \|\hat{\mathbf{d}}_i^S - \mathbf{u}_1\|^{-\beta_S}$ ,  $I_{T|S} = \sum_{\mathbf{d}_i^T \in \tilde{\mathcal{B}}_{T|S}} \bar{G}_T P_T X_i^T \|\hat{\mathbf{d}}_i^T - \mathbf{u}_1\|^{-\beta_T}$ , where  $\tilde{\mathcal{B}}_{S|S}$  ( $\tilde{\mathcal{B}}_{T|S}$ ) is the set of interfering satellites (terrestrial BSs) conditioned on that the typical user is connected to the satellite network. Based on (20), letting  $W$  be the operating bandwidth, the conditional achievable rate is given as  $R_{|S} = W \log_2(1 + \text{SINR}_{|S})$ . In the same manner, when the typical user is associated with the terrestrial network, the conditional SINR is given as

$$\text{SINR}_{|T} = \frac{G_T P_T X_1^T \|\hat{\mathbf{d}}_1^T - \mathbf{u}_1\|^{-\beta_T}}{I_{S|T} + I_{T|T} + \sigma^2}, \quad (21)$$

where  $I_{S|T} = \sum_{\mathbf{d}_i^S \in \tilde{\mathcal{B}}_{S|T}} \bar{G}_S P_S X_i^S \|\hat{\mathbf{d}}_i^S - \mathbf{u}_1\|^{-\beta_S}$ ,  $I_{T|T} = \sum_{\mathbf{d}_i^T \in \tilde{\mathcal{B}}_{T|T}} \bar{G}_T P_T X_i^T \|\hat{\mathbf{d}}_i^T - \mathbf{u}_1\|^{-\beta_T}$ . In turn, with the conditional achievable rate  $R_{|T} = W \log_2(1 + \text{SINR}_{|T})$ , the rate coverage probability is defined as

$$P^{\text{cov}}(\gamma, \lambda_o, \beta_o, m_o, f_{H_o}, P_o, B_o, G_o, \bar{G}_o, R_S, R_E) = \mathbb{P}[R_{\text{STIN}} > \gamma] \quad (22)$$

$$= \mathbb{P}[\mathcal{V}_S] \pi(S|\mathcal{V}_S) \mathbb{P}[R_{|S} > \gamma | o^* = S, \mathcal{V}_S] + \mathbb{P}[\mathcal{V}_T] \pi(T|\mathcal{V}_T) \mathbb{P}[R_{|T} > \gamma | o^* = T, \mathcal{V}_T], \quad (23)$$

where  $\pi(o|\mathcal{V}_o)$  indicates the probability that the typical user is associated with the network type  $o$  conditioned on that at least 1 point is visible in the network type  $o$ ,  $o \in \{S, T\}$ . Further, the visibility probabilities are

$$\mathbb{P}[\mathcal{V}_S] = \mathbb{P} \left[ \bigcup_{h \in \mathcal{H}_S} \{ \Phi_S^h(\mathcal{A}_{(R_S, h)}^i(r_{\max})) \geq 1 \} \right], \quad \mathbb{P}[\mathcal{V}_T] = \mathbb{P} \left[ \bigcup_{h \in \mathcal{H}_T} \{ \Phi_T^h(\mathcal{A}_{(R_E, h)}^i(r_{\max})) \geq 1 \} \right]. \quad (24)$$

**Remark 1.** [Rationale on random heights] Our model stands out because of its feature of assigning a random height to each point on the two spheres. This feature has two crucial implications. At first, our model is capable of reflecting more realistic scenarios. For instance, the existing network models for the satellite network [20], [21], [24] assumes that every satellite has the same altitude. This model, however, does not properly reflect the reality of satellite networks, as there are variations in the altitudes of individual satellites [1]. Further, in the terrestrial network, terrestrial BSs are installed on a structure such as rooftop or tower with different heights to ensure a wider coverage range. Our model is able to reflect these realistic situations.

Second, the random height is a key to unify the satellite network and the terrestrial network. As mentioned above, the satellite network has been modeled by using a spherical point process model [20], [21], [24], while planar point processes were mainly used for modeling terrestrial

networks [12], [15], [30]. To analyze STINs, it is of importance to combine these two disparate networks into one unified model. Although it may be tempting to adopt a spherical point process for both the satellite and terrestrial networks, this is infeasible. This is mainly because, when distributing points on the Earth to model spatial locations of terrestrial BSs, no terrestrial BS is mathematically visible from the typical user since no two points on a sphere can be connected via a straight line that does not intersect the sphere. By assigning random heights on points for terrestrial BSs, we ensure visibility, which makes it feasible to model the terrestrial network with a spherical point process. By doing this, we are able to capture the full complexity of the STIN into one unified analytical framework.

### III. MATHEMATICAL PRELIMINARIES

In this section, before delving into the rate coverage analysis, we present some necessary mathematical ingredients in this section. We start with the probability that at least 1 satellite is visible from the typical user.

**Lemma 1** (Visibility probability of the satellite network). *The number of visible satellites follows the Poisson distribution with parameter  $\lambda_S 2\pi R_S^2 \int_{h \in \mathcal{H}_S} \frac{h_S + h}{R_S + h} F_{H_S}(dh)$ . Hence, the probability that at least 1 satellite is visible at the typical user is*

$$\mathbb{P}[\mathcal{V}_S] = 1 - \exp \left( -\lambda_S 2\pi R_S^2 \int_{h \in \mathcal{H}_S} \frac{h_S + h}{R_S + h} F_{H_S}(dh) \right). \quad (25)$$

*Proof.* See Appendix A. □

**Corollary 1** (Visibility probability of the terrestrial network). *The number of visible terrestrial BS follows the Poisson distribution with parameter  $\lambda_S \lambda_T 2\pi R_E^2 \int_{h \in \mathcal{H}_T} \frac{h}{R_E + h} F_{H_T}(dh)$ . Hence, the probability that at least 1 terrestrial BS is visible at the typical user is*

$$\mathbb{P}[\mathcal{V}_T] = 1 - \exp \left( -\lambda_T 2\pi R_E^2 \int_{h \in \mathcal{H}_T} \frac{h}{R_E + h} F_{H_T}(dh) \right). \quad (26)$$

*Proof.* The proof is omitted since it is straightforward from Lemma 1. □

Now we derive the distribution of the nearest satellite distance conditioned on that at least 1 satellite is visible as follows.

**Lemma 2** (Conditional nearest satellite distance distribution). *Assume that the support of  $h$  of the satellite networks is  $\mathcal{H}_S = [h_S^{\min}, h_S^{\max}]$ . Defining the distance of the nearest satellite to the typical user as  $R$ , the PDF of  $R$  conditioned on the fact that at least 1 satellite is visible is*

$$f_R^S(r|\mathcal{V}_S) = \nu(\lambda_S, R_S) \cdot 2\pi\lambda_S r \cdot e^{-\lambda_S \int_{h_S^{\min}}^{h_S^{\max}} A_{R_S}(h,r) F_{H_S}(dh)}, \quad (27)$$

for  $R_{\min}^S \leq r \leq R_{\max}^S$  and 0 otherwise, where

$$\nu(\lambda_S, R_S) = \frac{\int_{h_S^{\min}}^{h_S^{\max}} \frac{R_S^2}{R_E(h+R_S)} F_{H_S}(dh) \cdot e^{-\lambda_S \int_{h_S^{\min}}^{h_S^{\max}} \frac{2\pi R_S^2(h_S+h)}{R_S+h} F_{H_S}(dh)}}{1 - \exp\left(-\lambda_S 2\pi R_S^2 \int_h \frac{h_S+h}{R_S+h} F_{H_S}(dh)\right)}, \quad (28)$$

and

$$A_{R_S}(h, r) = \begin{cases} 0, & r \leq R_S + h - R_E, \\ \frac{2\pi R_S^2 \left( h_S + h - \frac{(R_S+h)^2 - R_E^2 - r^2}{2R_E} \right)}{R_S+h}, & R_S + h - R_E \leq r \leq \sqrt{(R_S+h)^2 - R_E^2}, \\ \frac{2\pi R_S^2 (h_S+h)}{R_S+h}, & \sqrt{(R_S+h)^2 - R_E^2} \leq r, \end{cases} \quad (29)$$

and also

$$h_S^{\min} = \max\left(h_S^{\min}, \sqrt{r^2 + R_E^2} - R_S\right), \quad h_S^{\max} = \min(h_S^{\max}, r + R_E - R_S), \quad (30)$$

$$R_{\min}^S = R_S + h_S^{\min} - R_E, \quad R_{\max}^S = \sqrt{(R_S + h_S^{\max})^2 - R_E^2}. \quad (31)$$

*Proof.* See Appendix B. □

**Remark 2** (Reduction to the prior result). Assuming  $h = 0$  (i.e., all the satellites are on the given orbit with height  $h_S$ ), the conditional PDF (27) boils down to

$$f_R(r|\mathcal{V}_S) = \frac{2\pi\lambda_S \frac{R_S}{R_E} \exp\left(\lambda_S \pi \frac{R_S}{R_E} (R_S^2 - R_E^2)\right)}{\exp(\lambda_S 2\pi R_S (R_S - R_E)) - 1} r \exp\left(-\lambda_S \pi \frac{R_S}{R_E} r^2\right), \quad (32)$$

for  $R_{\min}^S \leq r \leq R_{\max}^S$ . We observe that (32) is a truncated Rayleigh distribution as shown in [24]. In this sense, Lemma 2 generalizes the prior result in [24].

Similar to the satellite network, we also derive the conditional distribution of the nearest terrestrial BS distance as follows.

**Corollary 2** (Conditional nearest terrestrial BS distance distribution). *Assume the support of  $h$  for the terrestrial networks of the form  $\mathcal{H}_T = [h_T^{\min}, h_T^{\max}]$ . Defining the distance of the nearest*

terrestrial BS to the typical user as  $R$ , the PDF of  $R$  conditioned on the fact that at least 1 terrestrial BS is visible is

$$f_R^T(r|\mathcal{V}_T) = \nu(\lambda_T, R_E) \cdot 2\pi\lambda_T r \cdot e^{-\lambda_T \int_{h_T^{low}}^{h_T^{high}} A_{R_E}(h,r) F_{H_T}(dh)}, \quad (33)$$

for  $R_{\min}^T \leq r \leq R_{\max}^T$  and 0 otherwise, where

$$\nu(\lambda_T, R_E) = \frac{\int_{h_T^{low}}^{h_T^{high}} \frac{R_E}{R_E+h} F_{H_T}(dh) \times e^{-\lambda_S \int_{h_T^{\min}}^{h_T^{low}} \frac{2\pi h}{R_E+h} R_E^2 F_{H_T}(dh)}}{1 - \exp\left(-\lambda_T 2\pi R_E^2 \int_h \frac{h}{R_E+h} F_{H_T}(dh)\right)}, \quad (34)$$

and

$$A_{R_E}(h, r) = \begin{cases} 0, & r \leq h, \\ \frac{2\pi R_E^2 \left( h - \frac{(R_E+h)^2 - R_E^2 - r^2}{2R_E} \right)}{R_E+h}, & h \leq r \leq \sqrt{h(h+2R_E)}, \\ \frac{2\pi h R_E^2}{R_E+h}, & \sqrt{h(h+2R_E)} \leq r, \end{cases} \quad (35)$$

and also

$$h_T^{low} = \max\left(h_T^{\min}, \sqrt{r^2 + R_E^2} - R_E\right), \quad h_T^{high} = \min(h_T^{\max}, r), \quad (36)$$

$$R_{\min}^T = h_T^{\min}, \quad R_{\max}^T = \sqrt{h_T^{\max}(h_T^{\max} + 2R_E)}. \quad (37)$$

*Proof.* The proof is omitted since it is straightforward from Lemma 2.  $\square$

Next, using the acquired conditional nearest distance probabilities, we obtain the probability that the typical user is associated with the satellite network conditioned on the fact that at least 1 satellite is visible, i.e.,  $\pi(S|\mathcal{V}_S)$ .

**Lemma 3** (Conditional association probability of the satellite network). *Under the condition that the typical user observes at least 1 satellite, the probability that the typical user is connected to the satellite network is given by*

$$\pi(S|\mathcal{V}_S) = \int_{R_{\min}^S}^{R_{\max}^S} f_R^S(r|\mathcal{V}_S) \cdot e^{-\lambda_T \int_{h \in \mathcal{H}_T} A_{R_E}\left(h, \left(\frac{P_T B_T}{P_S B_S}\right)^{\frac{1}{\beta_T}} r^{\frac{\beta_S}{\beta_T}}\right) F_{H_T}(dh)} dr. \quad (38)$$

*Proof.* See Appendix C.  $\square$

By exploiting this, we get the following result on the nearest satellite distance conditioned on that the typical user is associated with the satellite network:

**Lemma 4** (The conditional nearest satellite distance under the satellite association). *Conditioned on the fact that the typical user is associated with the satellite network, the nearest satellite distance PDF is given by*

$$f_R^S(r|\mathcal{V}_S, \{o^* = S\}) = \frac{f_R^S(r|\mathcal{V}_S) \cdot e^{-\lambda_T \int_{h \in \mathcal{H}_T} A_{R_E} \left( h, \left( \frac{P_T B_T}{P_S B_S} \right)^{\frac{1}{\beta_T}} r^{\frac{\beta_S}{\beta_T}} \right) F_{H_T}(dh)}}{\mathbb{P}[\mathcal{V}_S] \cdot \pi(S|\mathcal{V}_S)}, \quad (39)$$

where  $\mathbb{P}[\mathcal{V}_S]$  is given in (25) and  $\pi(S|\mathcal{V}_S)$  in (38).

*Proof.* The event that the nearest satellite distance is larger than  $r$  is equivalent to

$$\begin{aligned} \mathbb{P}[R > r|\mathcal{V}_S, \{o^* = S\}] &= \frac{\mathbb{P}[\bigcap_{h \in \mathcal{H}_S} \{\Phi_S^h(\mathcal{A}_{(R_S, h)}(r)) = 0\}, \mathcal{V}_S, \{o^* = S\}]}{\mathbb{P}[\mathcal{V}_S] \cdot \pi(S|\mathcal{V}_S)} \\ &= \frac{\int_r^{R_{\max}^S} f_R^S(v|\mathcal{V}_S) \cdot e^{-\lambda_T \int_{h \in \mathcal{H}_T} A_{R_E} \left( h, \left( \frac{P_T B_T}{P_S B_S} \right)^{\frac{1}{\beta_T}} v^{\frac{\beta_S}{\beta_T}} \right) F_{H_T}(dh)} dv}{\mathbb{P}[\mathcal{V}_S] \cdot \pi(S|\mathcal{V}_S)}. \end{aligned} \quad (40)$$

The corresponding PDF is obtained by differentiating (40) with regard to  $r$ .  $\square$

For conciseness, we present both the association probability of the terrestrial network and the conditional PDF of the nearest terrestrial BS's distance in the following corollary.

**Corollary 3** (Terrestrial network associated probabilities). *Under the condition that the typical user observes at least 1 terrestrial BS, the probability that the typical user is connected to the terrestrial network is*

$$\pi(T|\mathcal{V}_T) = \int_{R_{\min}^T}^{R_{\max}^T} f_R^T(r|\mathcal{V}_T) \cdot e^{-\lambda_S \int_{h \in \mathcal{H}_S} A_{R_S} \left( h, \left( \frac{P_S B_S}{P_T B_T} \right)^{\frac{1}{\beta_S}} r^{\frac{\beta_T}{\beta_S}} \right) F_{H_S}(dh)} dr. \quad (41)$$

*Conditioned on that the typical user is associated with the terrestrial network, the nearest terrestrial BS's distance PDF is given by*

$$f_R^T(r|\mathcal{V}_T, \{o^* = T\}) = \frac{f_R^T(r|\mathcal{V}_T) \cdot e^{-\lambda_S \int_{h \in \mathcal{H}_S} A_{R_S} \left( h, \left( \frac{P_S B_S}{P_T B_T} \right)^{\frac{1}{\beta_S}} r^{\frac{\beta_T}{\beta_S}} \right) F_{H_S}(dh)}}{\mathbb{P}[\mathcal{V}_T] \cdot \pi(T|\mathcal{V}_T)}, \quad (42)$$

where  $\mathbb{P}[\mathcal{V}_T]$  is given (26) and  $\pi(S|\mathcal{V}_S)$  in (41).

*Proof.* It is straightforward from the satellite network case. Due to the space limitation, we omit the proof.  $\square$

Finally, we obtain the Laplace transform of the aggregated interference power under the condition that the distances between the typical user and the interference sources are larger than  $r$ . The results are gathered in the following lemma.



**Lemma 5** (Conditional Laplace transforms of the aggregated interference power). *Under the condition that the distance between the typical user and the interfering satellites is larger than  $r$ , the conditional Laplace transform of the aggregated satellites' interference power is*

$$\mathcal{L}_{I_S}(s|r) = \exp \left( -2\pi\lambda_S \frac{R_S^2}{R_E} \int_{h \in \mathcal{H}_S} \frac{f_{H_S}(h)}{(h + R_S)} \cdot \left( \eta \left( \beta_S, m_S, \bar{G}_S P_S s, \sqrt{(R_S + h)^2 - R_E^2} \right) - \eta \left( \beta_S, m_S, \bar{G}_S P_S s, \min(\max(r, R_S - R_E + h), \sqrt{(R_S + h)^2 - R_E^2}) \right) \right) dh \right), \quad (43)$$

where

$$\eta(\beta, m, s, x) = \frac{x^2}{2} \left[ 1 - {}_2F_1 \left( -\frac{2}{\beta}, m; \frac{\beta - 2}{\beta}; -\frac{s x^{-\beta}}{m} \right) \right]. \quad (44)$$

Note that  ${}_2F_1(\cdot, \cdot; \cdot; \cdot)$  is the Gauss-hypergeometric function defined as

$${}_2F_1(a, b; c; z) = \frac{\Gamma(c)}{\Gamma(b)\Gamma(c-b)} \int_0^1 \frac{t^{b-1}(1-t)^{c-b-1}}{(1-tz)^a} dt. \quad (45)$$

Under the condition that the distance between the typical user and the interfering terrestrial BS is larger than  $r$ , the conditional Laplace transform of the terrestrial BSs' interference power is

$$\mathcal{L}_{I_T}(s|r) = \exp \left( -2\pi\lambda_T R_E \int_{h \in \mathcal{H}_T} \frac{f_{H_T}(h)}{(h + R_E)} \cdot \left( \eta \left( \beta_T, m_T, \bar{G}_T P_T s, \sqrt{h(h + 2R_E)} \right) - \eta \left( \beta_T, m_T, \bar{G}_T P_T s, \min(\max(r, h), \sqrt{h(h + 2R_E)}) \right) \right) dh \right), \quad (46)$$

*Proof.* See Appendix D. □

Now we are ready to obtain the rate coverage probability of the STIN.

#### IV. RATE COVERAGE ANALYSIS

Leveraging the presented mathematical preliminaries, we derive the rate coverage probability of the considered STIN in the following theorem.

**Theorem 1.** *In the considered STIN, the rate coverage probability is represented as*

$$\mathbb{P}[R_{\text{STIN}} > \gamma] = P^{\text{cov}}(\gamma, \lambda_o, \beta_o, m_o, f_{H_o}, P_o, B_o, G_o, \bar{G}_o, R_S, R_E) = P_S^{\text{cov}} + P_T^{\text{cov}}, \quad (47)$$

where  $P_S^{\text{cov}}$  is

$$P_S^{\text{cov}} = P_{\mathcal{V}_S} \cdot \pi(\mathcal{S}|\mathcal{V}_S) \cdot \int_{R_{\min}^S}^{R_{\max}^S} f_R^S(r|\mathcal{V}_S, \{o^* = \mathcal{S}\}) \cdot \sum_{k=1}^{m_S-1} \frac{m_S^k r^{k\beta_S} \tilde{\gamma}^k}{k!} (-1)^k \frac{\partial^k \mathcal{L}_{I_S} \left( \frac{s}{G_S P_S} | r \right) \cdot \mathcal{L}_{I_T} \left( \frac{s}{G_S P_S} \left| \left( \frac{P_T B_T}{P_S B_S} \right)^{\frac{1}{\beta_T}} r^{\frac{\beta_S}{\beta_T}} \right. \right) \cdot \exp \left( -s \tilde{\sigma}_{|S}^2 \right)}{\partial s^k} \bigg|_{s=m_S \tilde{\gamma} r^{\beta_S}} dr, \quad (48)$$

where  $P_{\mathcal{V}_S} = \mathbb{P}[\mathcal{V}_S]$  is given in (25),  $\pi(\mathcal{S}|\mathcal{V}_S)$  in (38),  $f_R^S(r|\mathcal{V}_S, \{o^* = \mathcal{S}\})$  in (39), and  $\mathcal{L}_{I_S}(s|r)$  and  $\mathcal{L}_{I_T}(s|r)$  are given in (43) and (46), respectively. Meanwhile,  $P_T^{\text{cov}}$  is

$$P_T^{\text{cov}} = P_{\mathcal{V}_T} \cdot \pi(\mathcal{T}|\mathcal{V}_T) \cdot \int_{R_{\min}^T}^{R_{\max}^T} f_R^T(r|\mathcal{V}_T, \{o^* = \mathcal{T}\}) \cdot \sum_{k=1}^{m_T-1} \frac{m_T^k r^{k\beta_T} \tilde{\gamma}^k}{k!} (-1)^k \frac{\partial^k \mathcal{L}_{I_S} \left( \frac{s}{G_T P_T} \left| \left( \frac{P_S B_S}{P_T B_T} \right)^{\frac{1}{\beta_S}} r^{\frac{\beta_T}{\beta_S}} \right. \right) \cdot \mathcal{L}_{I_T} \left( \frac{s}{G_T P_T} | r \right) \cdot \exp \left( -s \tilde{\sigma}_{|T}^2 \right)}{\partial s^k} \bigg|_{s=m_T \tilde{\gamma} r^{\beta_T}} dr, \quad (49)$$

where  $P_{\mathcal{V}_T} = \mathbb{P}[\mathcal{V}_T]$  is given in (26),  $\pi(\mathcal{T}|\mathcal{V}_T)$  in (41),  $f_R^T(r|\mathcal{V}_T, \{o^* = \mathcal{T}\})$  in (42), and  $\mathcal{L}_{I_S}(s|r)$  and  $\mathcal{L}_{I_T}(s|r)$  are given in (43) and (46), respectively.

*Proof.* See Appendix E. □

**Remark 3** (Upper/lower bounds and Rayleigh assumption). As in Theorem 2 of [24], we can obtain tractable upper/lower bounds on the rate coverage probability (47) using Alzer's inequality [31]. For instance, bounds on (48) are given by

$$P_{S,B}^{\text{cov}}(\kappa_S) = P_{\mathcal{V}_S} \cdot \pi(\mathcal{S}|\mathcal{V}_S) \cdot \int_{R_{\min}^S}^{R_{\max}^S} f_R^S(r|\mathcal{V}_S, \{o^* = \mathcal{S}\}) \cdot \sum_{\ell=1}^{m_S} \binom{m_S}{\ell} (-1)^{\ell+1} \mathcal{L}_{I_S} \left( \frac{\ell m_S \kappa_S r^{\beta_S} \tilde{\gamma}}{G_S P_S} \middle| r \right) \mathcal{L}_{I_T} \left( \frac{\ell m_S \kappa_S r^{\beta_S} \tilde{\gamma}}{G_S P_S} \left| \left( \frac{P_T B_T}{P_S B_S} \right)^{\frac{1}{\beta_T}} r^{\frac{\beta_S}{\beta_T}} \right. \right) \exp \left( -\frac{\ell m_S \kappa_S r^{\beta_S} \tilde{\gamma}}{G_S P_S} \sigma_{|S}^2 \right) dr, \quad (50)$$

where  $\kappa_S = (m_S!)^{\frac{1}{m_S}}$  produces a lower bound and  $\kappa_S = 1$  produces an upper bound. We do not include more details in this paper due to the space limitation, yet one can follow the process of Theorem 2 in [24] to reach the upper and lower bounds.

We can further simplify the rate coverage expressions in Theorem 1 by assuming Rayleigh fading for both of the satellite links and the terrestrial links, i.e.,  $m_S = 1$  and  $m_T = 1$ . We note that, however, the Rayleigh fading assumption does not perfectly fit with the reality, especially

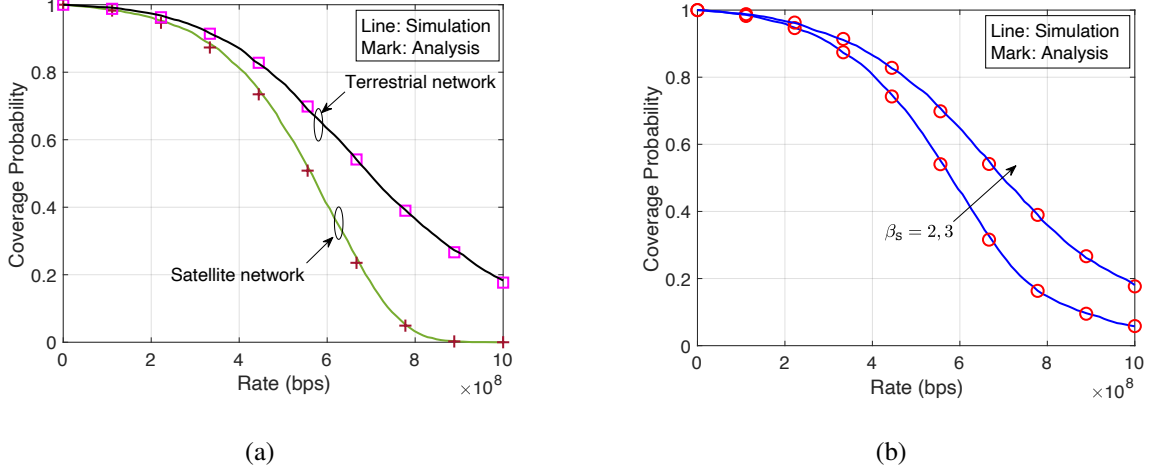


Fig. 3: Validation of the rate coverage analysis. The used system parameters:  $\beta_S = 2$ ,  $\beta_T = 4$ ,  $\bar{N}_S = 100$ ,  $\bar{N}_T = 5000$ ,  $[h_S^{\min}, h_S^{\max}] = [0, 1000]$ ,  $f_{H_S}(h) = \text{Unif}([h_S^{\min}, h_S^{\max}])$ ,  $[h_T^{\min}, h_T^{\max}] = [0, 200]$ ,  $f_{H_T}(h) = \text{Unif}([h_T^{\min}, h_T^{\max}])$ ,  $P_S = 43\text{dBm}$ ,  $P_T = 46\text{dBm}$ ,  $W = 100\text{MHz}$ ,  $N_0 = -174\text{dBm/Hz}$ ,  $G_S = 20\text{dBi}$ ,  $\bar{G}_S = -10\text{dBi}$ ,  $G_T = 10\text{dBi}$ ,  $\bar{G}_T = -10\text{dBi}$ ,  $B_T = 1$ ,  $B_S = 10$ ,  $R_E = 6371\text{km}$ ,  $h_S = 500\text{km}$  (unless mentioned otherwise in the figure).

with satellite communications. This is because, the satellite communication links are likely to be LoS due to the scarcity of scatters in the space [20], [24]. Additionally, the terrestrial communication links can also be LoS depending on the propagation environments and operating bandwidth [14]. Nonetheless, the Rayleigh fading assumption has been popularly adopted in the stochastic geometry literature even when studying LoS communications [15], [32]–[34], rationalized by the fact that it offers significant tractability while not hurting a major trend of the coverage performance as demonstrated in [15], [32], [33]. In the same spirit, we use the Rayleigh fading assumption in the remaining part of the paper by taking  $m_S = 1$  and  $m_T = 1$ .

Now we verify the obtained rate coverage probability by comparing with the simulation results. This is done in Fig. 3, which includes the used system parameters in its caption. As shown in Fig. 3, Theorem 1 and the rate coverage probability obtained by numerical simulations are perfectly matched. For a more thorough validation, we also check the individual rate coverage of the terrestrial network and the satellite network separately, and observe that the simulation results and the analysis also match.

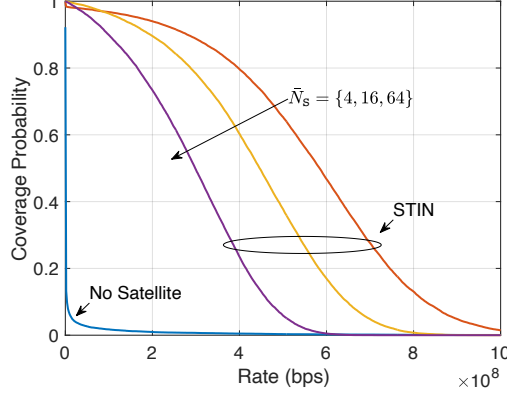


Fig. 4: Coverage extension in the STIN. The used system parameters:  $\beta_S = 2$ ,  $\beta_T = 4$ ,  $\bar{N}_S = \{4, 16, 64\}$ ,  $\bar{N}_T = 5$ ,  $[h_S^{\min}, h_S^{\max}] = [0, 1000]$ ,  $f_{H_S}(h) = \text{Unif}([h_S^{\min}, h_S^{\max}])$ ,  $[h_T^{\min}, h_T^{\max}] = [0, 200]$ ,  $f_{H_T}(h) = \text{Unif}([h_T^{\min}, h_T^{\max}])$ ,  $P_S = 43\text{dBm}$ ,  $P_T = 46\text{dBm}$ ,  $W = 100\text{MHz}$ ,  $N_0 = -174\text{dBm/Hz}$ ,  $G_S = 10\text{dBi}$ ,  $\bar{G}_S = -10\text{dBi}$ ,  $G_T = 0\text{dBi}$ ,  $\bar{G}_T = 0\text{dBi}$ ,  $B_T = 1$ ,  $B_S = 1$ ,  $R_E = 6371\text{km}$ ,  $h_S = 500\text{km}$ .

## V. STIN BENEFITS STUDY: COVERAGE EXTENSION AND DATA OFFLOADING

Leveraging the derived analytical results, we explore the benefits that STINs provide in two different scenarios: coverage extension in remote rural areas and data offloading in dense urban areas.

### A. Coverage Extension in Remote Rural Areas

The deployment density of the terrestrial network is often limited in remote rural areas such as a desert or a deep mountain valley, resulting in users being left outside of coverage regions. In contrast to that, the satellite network provides a relatively consistent density as each satellite continues to move along a given orbit around the Earth. This is where the STIN is particularly useful, as it can provide coverage to the users experiencing outages in the terrestrial network. Our analysis can show how the coverage extension benefits by comparing the rate coverage performances between the scenario where only the terrestrial network is used and the STIN scenario. We illustrate this comparison in Fig. 4, whose caption includes the detailed system parameters.

Fig. 4 demonstrates significant improvements in the rate coverage by using the STIN. When  $\lambda_T$  is low ( $\bar{N}_T = 5$ ), the median rate (i.e., the coverage probability that 50% of users can achieve)

is 0bps when only the terrestrial network is deployed, while the STIN with  $\bar{N}_S = \{4, 16, 64\}$  achieves the median rate  $\{5.8, 4.4, 2.9\} \times 10^8 \text{bps}$ . This implies that, a user experiencing outage can have 0.59Gbps with 50% chance by integrating the terrestrial network and the satellite network with  $\bar{N}_S = 4$  (4 visible satellites on average). It is important to mention that the rate coverage of the STIN decreases as the satellite density increases. This is because when the satellite density increases, the amount of interference also increases. This observation is aligned with the findings of [24]. For this reason, to attain the optimum coverage extension benefits from the STIN, it is essential to use a proper number of the satellites.

### B. Data Offloading in Dense Urban Areas

In dense urban areas where the data traffic load is high, the terrestrial network can suffer from scarcity of the available wireless resources. In the STIN situation, the satellite network is capable of relieving the traffic by data offloading. To capture this, adopting the approach used in HetNets [10], [11], we first redefine the rate by incorporating the load as follows:

$$R_{|o} = \frac{W_{\text{tot}}}{L_o} \log(1 + \text{SINR}_{|o}), \quad (51)$$

where  $L_o$  is the load associated with the network type  $o$  with  $o \in \{\text{T}, \text{S}\}$ . Inspired by the mean load characterization in [10], we approximate the load as follows:

$$L_S = 1 + \frac{\lambda_U \pi(S|\mathcal{V}_S)}{\lambda_S}, \quad L_T = 1 + \frac{\lambda_U \pi(T|\mathcal{V}_T)}{\lambda_T}. \quad (52)$$

We clarify that (52) is an approximation, not an exact form. Characterizing the load of the STIN in an exact form is very challenging since it requires to obtain the Poisson-Voronoi cell area distribution [35] in 3D finite spherical models. It is definitely interesting future work.

Notwithstanding an approximation, the offloading effects are properly captured in (52). For instance, assume  $B_S$  increases. Then, as given by (19), the typical user is more likely to be associated to the satellite network ( $\pi(S|\mathcal{V}_S)$  increases), by which the data traffic is pushed to the satellite network. Accordingly,  $L_S$  increases while  $L_T$  decreases; resulting in that the available resources in the terrestrial network increase. Now, assume  $\lambda_S$  increases. Then the number of users served per satellite decreases, which relieves  $L_S$  in (52). Nonetheless, this does not necessarily increase the rate coverage since the SINR of the satellite network sharply degrades as  $\lambda_S$  increases due to the increased amount of interference as observed in Fig. 4.

We explore data offloading in the STIN by describing the 10th-percentile rate (the rate coverage probability that 90% of users can achieve) in Fig. 5 depending on the bias factor  $B_S$  and the

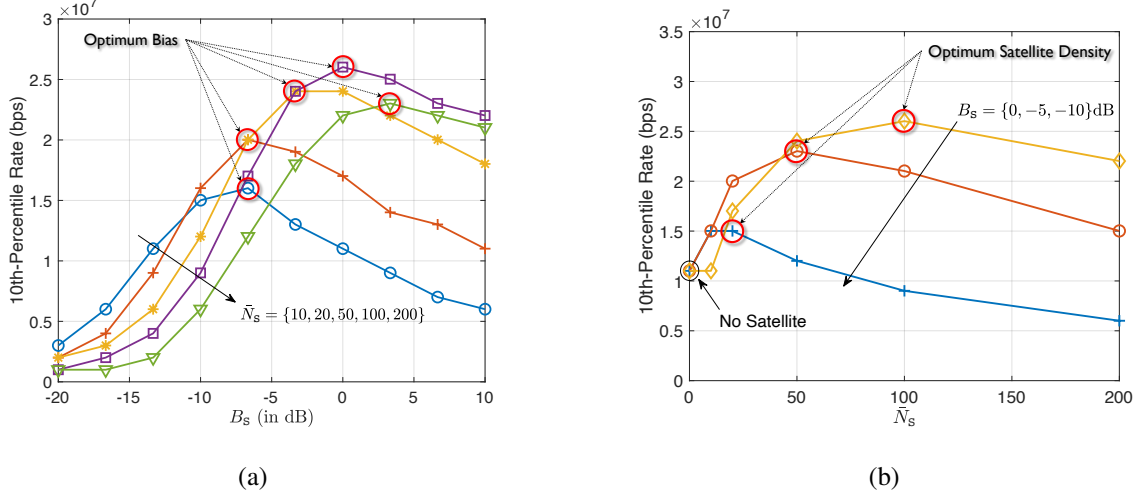


Fig. 5: 10th-percentile rate per bias ( $B_S$ ) and satellite density ( $\bar{N}_S$ ) to observe offloading in the STIN. The used system parameters are same with Fig.4, unless mentioned otherwise in the figure.

satellite density  $\lambda_S$  (or  $\bar{N}_S$ ). In Fig. 5-(a), we see the optimum bias factor  $B_S^*$  for different satellite density scenarios. For example, if  $\bar{N}_S = 10$ , the optimum bias is  $B_S^* = -6.6$ dB, while if  $\bar{N}_S = 100$ , the optimum bias is  $B_S^* = 0$ dB. Generally, the optimum bias is proportional to the satellite density. This is reasonable because if sufficiently many satellites are deployed, it is advantageous to push the data traffic to the satellite network. In Fig. 5-(b), we draw the 10th-percentile rate per satellite density. Provided that proper bias is used, the rate coverage performance is proportional to the satellite density, which is in sharp contrast to Fig. 4 and [24]. This is because, as the satellite density increases, the available resources of the satellite network  $W_{\text{tot}}/L_S$  increase as  $L_S$  diminishes. Meanwhile,  $\text{SINR}_{|S}$  decreases since the amount of interference increases. In turn, by incorporating the load  $L_S$ , we have a trade-off in the rate coverage (51) with regard to  $\lambda_S$ . In the regime drawn in Fig. 5, the load has a dominant effect, so relieving the load even by sacrificing the SINR helps to improve the rate coverage performance.

To further investigate the trade-off of the rate coverage performance, we illustrate the 10th-percentile rate per user density  $\lambda_U$  in Fig. 6. If  $\lambda_U$  is small, then  $L_o \rightarrow 1$  so that the offloading effect becomes negligible. In this regime, the SINR is dominant to determine the rate, thereby the rate coverage performance decreases as the satellite density increases. This is shown in Fig. 6, where this regime is referred to the SINR-limited regime. In contrast, if  $\lambda_U$  is high, the offloading

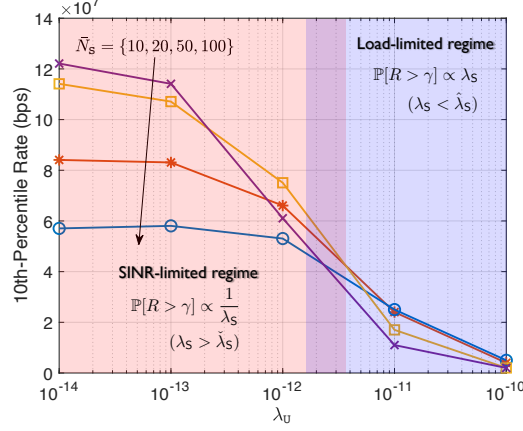


Fig. 6: Rate coverage trend in the SINR-limited regime vs. the load-limited regime.

effect becomes significant, so the load  $L_o$  is dominant for the rate. Accordingly, the rate coverage performance is proportional to the satellite density. We call this regime the load-limited regime, as presented in Fig. 6. We note that even in the SINR-limited regime, the rate coverage does not monotonically increase as the satellite density decreases. Specifically, if  $\lambda_S \rightarrow 0$ , no satellite is visible to the typical user, so that the rate coverage decreases as depicted in Fig. 4. For this reason, there exists a threshold  $\tilde{\lambda}_S$  such that  $\mathbb{P}[R_{\text{STIN}} > \gamma] \propto 1/\lambda_S$  when  $\lambda_S > \tilde{\lambda}_S$ . This is also the case of the load-limited regime, i.e.,  $\mathbb{P}[R_{\text{STIN}} > \gamma] \propto \lambda_S$  when  $\lambda_S < \hat{\lambda}_S$ .

Due to the contrasting behavior of the SINR-limited regime and the load-limited regime, it is essential to identify the operating regime of the STIN in order to achieve optimum performance gains. For instance, in the SINR-limited regime, integrating more satellites into the STIN only degrades the rate coverage performance. In contrast, in the load-limited regime, it is beneficial to include more satellites into the STIN for more active data offloading.

## VI. CONCLUSIONS

In this paper, we have developed a unified modeling for the two components of a STIN. Our key idea for capturing both of the satellite network and the terrestrial network into one framework is distributing PPPs on spheres and assigning random heights. Based on this model, we have derived the rate coverage probability as a function of the key system parameters, chiefly the densities, path-loss exponents, height geometries (maximum/minimum altitudes and height distributions), and bias factors of the satellites and the terrestrial BSs. Leveraging the analysis, we have explored the two benefits of the STIN: coverage extension in remote rural areas and data

offloading in dense urban areas. Through this, we have extracted valuable system design insights:

- 1) In remote rural areas, the STIN significantly increases the rate coverage performance; yet to obtain this, it is necessary to carefully choose the satellite density.
- 2) In dense urban areas, the STIN helps to offload the data traffic from the terrestrial BSs, provided that the satellite density and the bias are properly selected.
- 3) The STIN has two contrasting operating regimes; the SINR-limited regime where increasing the satellite density degrades the rate coverage, and the load-limited regime where increasing the satellite density improves the rate coverage. For efficiently operating a STIN, it is needed to carefully identify the appropriate operation regime.

## APPENDIX A

### PROOF OF LEMMA 1

We first recall that satellite at  $\hat{\mathbf{d}}_i^S$  (with height  $h$ ) is visible at the typical user if and only if  $\mathbf{d}_i^S \in \mathcal{A}_{(R_S, h)}^i(r_{\max})$  (or equivalently  $\hat{\mathbf{d}}_i^S \in \mathcal{A}_{(R_S, h)}^o(r_{\max})$ ). For simplicity, we write  $\mathcal{A}(h) = \mathcal{A}_{(R_S, h)}^i(r_{\max})$ . Let  $N = \sum_i \mathbf{1}\{\mathbf{d}_i^S \in \mathcal{A}(h_i)\}$  where  $h_i$  is the height of satellite at  $\mathbf{d}_i^S$ , then  $N_v$  represents the number of visible satellites. For  $0 \leq z \leq 1$ , the probability generating function (PGF) of  $N$  is

$$\mathbb{E}[z^N] = \mathbb{E}\left[e^{\sum_i \ln z \mathbf{1}\{\mathbf{d}_i^S \in \mathcal{A}(h_i)\}}\right] \stackrel{(a)}{=} \exp\left(-\int_{h \in \mathcal{H}_S} \int_{x \in \mathcal{A}(h)} (1-z) \mathbf{1}\{\mathbf{d}_i^S \in \mathcal{A}(h_i)\} \Phi_S(dx) F_{H_S}(dh)\right) \quad (53)$$

$$\begin{aligned} &= \exp\left(-\lambda_S(1-z) \int_{h \in \mathcal{H}_S} |\mathcal{A}(h)| F_{H_S}(dh)\right) \\ &= \exp\left(-\lambda_S(1-z) 2\pi R_S^2 \int_{h \in \mathcal{H}_S} \frac{h_S + h}{R_S + h} F_{H_S}(dh)\right), \end{aligned} \quad (54)$$

where (a) comes from the Laplace functional of an independently marked PPP and  $F_{H_S}$  is the CDF of satellite height  $H_S$ . Hence  $N$  is Poisson with parameter  $\lambda_S 2\pi R_S^2 \int_{h \in \mathcal{H}_S} \frac{h_S + h}{R_S + h} F_{H_S}(dh)$ , we have

$$\mathbb{P}[N = 0] = \exp\left(-\lambda_S 2\pi R_S^2 \int_{h \in \mathcal{H}_S} \frac{h_S + h}{R_S + h} F_{H_S}(dh)\right). \quad (55)$$

This completes the proof.

## APPENDIX B

### PROOF OF LEMMA 2

Denoting  $R$  by the nearest satellite distance to the typical user, the event  $R > r$  is equivalent to the event that there is no satellite with a height  $h$  in  $\mathcal{A}_{(R_S, h)}^i(r)$ . Denoting  $\Phi_S^h$  as a set of



satellites with height  $h$ , we represent the CCDF of  $R$  conditioned on the fact that at least 1 satellite is visible to the typical user as

$$F_{R|\{\mathcal{V}_S\}}^c(r) = \mathbb{P}[R > r|\mathcal{V}_S] \stackrel{(a)}{=} \frac{\mathbb{P}\left[\bigcap_{h \in \mathcal{H}_S} \{\Phi_S^h(\mathcal{A}_{(R_S, h)}^i(r)) = 0\}\right] \cdot (1 - \mathbb{P}[\bigcap_{h \in \mathcal{H}_S} \Phi_S^h(\mathcal{A}_{(R_S, h)}^i(r_{\max}) \setminus \mathcal{A}_{(R_S, h)}^i(r)) = 0])}{\mathbb{P}[\mathcal{V}_S]} \quad (56)$$

where (a) follows from the fact that the PPP in  $\mathcal{A}_{(R_S, h)}^i(r)$  and  $\mathcal{A}_{(R_S, h)}^i(r_{\max}) \setminus \mathcal{A}_{(R_S, h)}^i(r)$  are independent since their sets do not overlap. Now we compute the first term in the numerator of (56) as

$$\mathbb{P}\left[\bigcap_{h \in \mathcal{H}_S} \{\Phi_S^h(\mathcal{A}_{(R_S, h)}^i(r)) = 0\}\right] = \prod_{h \in \mathcal{H}_S} \mathbb{P}[\Phi_S^h(\mathcal{A}_{(R_S, h)}^i(r)) = 0] \quad (57)$$

$$= \prod_{h \in \mathcal{H}_S} \exp(-\lambda_S f_{H_S}(h) \Delta h A_{R_S}(h, r)) = \exp\left(-\lambda_S \int_{h \in \mathcal{H}_S} A_{R_S}(h, r) F_{H_S}(dh)\right), \quad (58)$$

where  $A_{R_S}(h, r)$  is an area function of  $\mathcal{A}_{(R_S, h)}^i(r)$  made feasible for the whole region of  $r$ , defined as (29). The second term in the numerator of (56) is

$$\mathbb{P}\left[\bigcap_{h \in \mathcal{H}_S} \Phi_S^h(\mathcal{A}_{(R_S, h)}^i(r_{\max}) \setminus \mathcal{A}_{(R_S, h)}^i(r)) = 0\right] = \exp\left(-\lambda_S \int_{h \in \mathcal{H}_S} (A_{R_S}(h, r_{\max}) - A_{R_S}(h, r)) F_{H_S}(dh)\right), \quad (59)$$

where  $A_{R_S}(h, r)$  is (29). Now we put (58) and (59) together, which leads to

$$\mathbb{P}[R > r|\mathcal{V}_S] = \frac{\left\{ \begin{array}{l} \exp\left(-\lambda_S \int_h A_{R_S}(h, r) F_{H_S}(dh)\right) \cdot \\ [1 - \exp\left(-\lambda_S \int_h (A_{R_S}(h, r_{\max}) - A_{R_S}(h, r)) F_{H_S}(dh)\right)] \end{array} \right\}}{1 - \exp\left(-\lambda_S 2\pi R_S^2 \int_h \frac{h_S + h}{R_S + h} F_{H_S}(dh)\right)}. \quad (60)$$

We finally derive the conditional PDF. Since the conditional PDF is obtained by taking derivative to the conditional CDF regarding  $r$ , we have

$$f_{R|\{\mathcal{V}_S\}}^S(r) = \frac{\partial F_{R|\{\mathcal{V}_S\}}(r)}{\partial r} = \frac{\lambda_S \int_h A'_{R_S}(h, r) F_{H_S}(dh) \cdot e^{-\lambda_S \int_h A_{R_S}(h, r) F_{H_S}(dh)}}{1 - \exp\left(-\lambda_S 2\pi R_S^2 \int_h \frac{h_S + h}{R_S + h} F_{H_S}(dh)\right)}, \quad (61)$$

where  $A'_{R_S}(h, r)$  is the derivative of  $A_{R_S}(h, r)$  with regard to  $r$  obtained as

$$A'_{R_S}(h, r) = \frac{\partial A_{R_S}(h, r)}{\partial r} = \frac{2\pi r R_S^2}{R_E(h + R_S)}, \quad (62)$$

if  $R_S + h - R_E \leq r \leq \sqrt{(R_S + h)^2 - R_E^2}$  and  $A'_{R_S}(h, r) = 0$  otherwise. Plugging (62) into (61), we reach

$$\frac{\lambda_S \int_{h_S^{\text{low}}}^{h_S^{\text{high}}} \frac{2\pi r R_S^2}{R_E(h + R_S)} F_{H_S}(dh)}{1 - \exp\left(-\lambda_S 2\pi R_S^2 \int_h \frac{h_S + h}{R_S + h} F_{H_S}(dh)\right)} e^{-\lambda_S \int_{h_S^{\text{low}}}^{h_S^{\text{high}}} A_{R_S}(h, r) F_{H_S}(dh)} e^{-\lambda_S \int_{h_S^{\text{min}}}^{h_S^{\text{low}}} \frac{2\pi R_S^2 (h_S + h)}{R_S + h} F_{H_S}(dh)} \quad (63)$$

where  $h_S^{\text{low}}$  and  $h_S^{\text{high}}$  are defined in (30). Noting that the distance  $r$  can have a feasible range of  $R_{\min}^S \leq r \leq R_{\max}^S$  as defined in (31), we complete the proof.

## APPENDIX C

### PROOF OF LEMMA 3

The typical user is connected to the satellite network when a satellite provides the maximum reference signal power, i.e.,  $P_S B_S \|\hat{\mathbf{d}}_1^S - \mathbf{u}_1\|^{-\beta_S} > P_T B_T \|\hat{\mathbf{d}}_i^T - \mathbf{u}_1\|^{-\beta_T}, \hat{\mathbf{d}}_i^T \in \hat{\Phi}_T$ . Calculating the above probability, we get

$$\begin{aligned} & \mathbb{P} \left[ P_S B_S \|\hat{\mathbf{d}}_1^S - \mathbf{u}_1\|^{-\beta_S} > P_T B_T \|\hat{\mathbf{d}}_i^T - \mathbf{u}_1\|^{-\beta_T}, \hat{\mathbf{d}}_i^T \in \hat{\Phi}_T \right] \\ &= \mathbb{E}_R \left[ \mathbb{P} \left[ \left( \frac{P_T B_T}{P_S B_S} \right)^{\frac{1}{\beta_T}} R^{\frac{\beta_S}{\beta_T}} < \|\hat{\mathbf{d}}_i^T - \mathbf{u}_1\|, \hat{\mathbf{d}}_i^T \in \hat{\Phi}_T \mid R \right] \right]. \end{aligned} \quad (64)$$

The inner probability of (64) is equivalent to the probability that there is no terrestrial BS whose distance to the typical user is smaller than  $\left( \frac{P_T B_T}{P_S B_S} \right)^{\frac{1}{\beta_T}} R^{\frac{\beta_S}{\beta_T}}$ . We compute this as follows. Denoting that a set of terrestrial BSs whose heights are in  $[h, h + \Delta h]$  as  $\hat{\Phi}_T^h \subset \hat{\Phi}_T$  and  $\Phi_T^h \subset \Phi_T$ ,  $\hat{\Phi}_T^h$  is a homogeneous PPP with the density of  $\lambda_T^h = \lambda_T (F_{H_T}(h + \Delta h) - F_{H_T}(h)) = \lambda_T f_{H_T}(h) \Delta h$ , where  $\Delta h \rightarrow 0$ . Further,  $\hat{\Phi}_T^{h_1}$  and  $\hat{\Phi}_T^{h_2}$  are statistically independent if  $h_1 \neq h_2$ . Hence, for given  $R$ , the inner probability of (64) is

$$\begin{aligned} & \mathbb{P} \left[ \bigcap_{h \in \mathcal{H}_T} \left\{ \Phi_T^h \left( \mathcal{A}_{(R_E, h)}^i \left( \left( \frac{P_T B_T}{P_S B_S} \right)^{\frac{1}{\beta_T}} R^{\frac{\beta_S}{\beta_T}} \right) \right) = 0 \right\} \right] \\ &= \prod_{h \in \mathcal{H}_T} \exp \left( -\lambda_T f_{H_T}(h) \Delta h \left| \mathcal{A}_{(R_E, h)}^i \left( \left( \frac{P_T B_T}{P_S B_S} \right)^{\frac{1}{\beta_T}} R^{\frac{\beta_S}{\beta_T}} \right) \right| \right) \end{aligned} \quad (65)$$

$$= \exp \left( -\lambda_T \sum_{h \in \mathcal{H}_T} f_{H_T}(h) \Delta h A_{R_E}(h, r) \right) \stackrel{(a)}{=} \exp \left( -\lambda_T \int_h A_{R_E} \left( h, \left( \frac{P_T B_T}{P_S B_S} \right)^{\frac{1}{\beta_T}} R^{\frac{\beta_S}{\beta_T}} \right) F_{H_T}(dh) \right), \quad (66)$$

where (a) comes from Riemann integration with  $\Delta h \rightarrow 0$  and  $A_{R_E}(h, r)$  is an extended area function of  $\mathcal{A}_{(R_E, h)}^i(r)$  defined in (35). The final step is marginalizing (66) with regard to  $R$ . Since  $R$  is distributed as (27), we reach

$$\pi(S|\mathcal{V}_S) = \int_r \nu(\lambda_S, R_S) 2\pi \lambda_S r e^{-\lambda_S \int_{h_{\text{low}}}^{h_{\text{high}}} A_{R_S}(h, r) F_{H_S}(dh)} \cdot e^{-\lambda_T \int_h A_{R_E} \left( h, \left( \frac{P_T B_T}{P_S B_S} \right)^{\frac{1}{\beta_T}} r^{\frac{\beta_S}{\beta_T}} \right) F_{H_T}(dh)} dr. \quad (67)$$

This completes the proof.

## APPENDIX D

### PROOF OF LEMMA 5

Conditioned on that the distance to the interference source is larger than  $r$ , the aggregated satellite interference is  $I_S = \sum_{\|\hat{\mathbf{d}}_i^S - \mathbf{u}_1\| > r} \bar{G}_S P_S X_i^S \|\hat{\mathbf{d}}_i^S - \mathbf{u}_1\|^{-\beta_S}$ . We first note that the aggregated satellite interference can be further separated into  $I_S = \sum_{h \in \mathcal{H}_S} I_S^h$  where  $I_S^h$  represents the interference coming from the satellites with height  $h$  and  $\mathcal{A}_{(R_S, h)}^{i, c}(r) = \mathcal{A}_{(R_S, h)}^i(r_{\max}) \setminus \mathcal{A}_{(R_S, h)}^i(r)$ . We note that  $I_S^{h_1}$  and  $I_S^{h_2}$  are independent for  $h_1 \neq h_2$  due to independent thinning of a PPP. Accordingly, the conditional Laplace transform is written as

$$\mathcal{L}_{I_S}(s|r) = \mathbb{E} \left[ e^{-sI_S} \mid \|\hat{\mathbf{d}}_1^S - \mathbf{u}_1\| = r \right] = \prod_{h \in \mathcal{H}_S} \mathbb{E} \left[ e^{-sI_S^h} \mid \|\hat{\mathbf{d}}_1^S - \mathbf{u}_1\| = r \right]. \quad (68)$$

Then we have

$$\mathbb{E} \left[ e^{-sI_S^h} \mid \|\hat{\mathbf{d}}_1^S - \mathbf{u}_1\| = r \right] \stackrel{(a)}{=} \exp \left( -\lambda_S f_{H_S}(h) \Delta h \int_{v \in \mathcal{A}_{(R_S, h)}^{i, c}(r)} 1 - \mathbb{E} \left[ e^{-s\bar{G}_S P_S X_i^S v^{-\beta_S}} \right] dv \right) \quad (69)$$

$$\stackrel{(b)}{=} \exp \left( -\lambda_S f_{H_S}(h) \Delta h \int_{v \in \mathcal{A}_{(R_S, h)}^{i, c}(r)} 1 - \frac{1}{\left( 1 + \frac{s\bar{G}_S P_S v^{-\beta_S}}{m_S} \right)^{m_S}} dv \right) \quad (70)$$

$$\stackrel{(c)}{=} \exp \left( -\frac{\lambda_S f_{H_S}(h) 2\pi R_S^2 \Delta h}{R_E(h + R_S)} \int_{\min(\max(r, R_S - R_E + h), \sqrt{(R_S + h)^2 - R_E^2})}^{\sqrt{(R_S + h)^2 - R_E^2}} \left( 1 - \frac{1}{\left( 1 + \frac{s\bar{G}_S P_S v^{-\beta_S}}{m_S} \right)^{m_S}} \right) v dv \right), \quad (71)$$

where (a) comes from the probability generating functional (PGFL) of a PPP, (b) follows that  $X_i^S$  is distributed as the Gamma distribution, and (c) is because

$$\frac{\partial |\mathcal{A}_{(R_S, h)}^i(r)|}{\partial r} = \frac{2\pi r R_S^2}{R_E(h + R_S)}, \quad R_S - R_E + h \leq r \leq \sqrt{(R_S + h)^2 - R_E^2}. \quad (72)$$

Combining all  $h \in \mathcal{H}_S$ , we reach

$$\begin{aligned} \mathcal{L}_{I_S}(s|r) &= \\ &\exp \left( -2\pi \lambda_S \frac{R_S^2}{R_E} \int_{h \in \mathcal{H}_S} \frac{f_{H_S}(h)}{(h + R_S)} \int_{\min(\max(r, R_S - R_E + h), \sqrt{(R_S + h)^2 - R_E^2})}^{\sqrt{(R_S + h)^2 - R_E^2}} \left( 1 - \frac{1}{\left( 1 + \frac{s\bar{G}_S P_S v^{-\beta_S}}{m_S} \right)^{m_S}} \right) v dv dh \right) \\ &= \exp \left( -2\pi \lambda_S \frac{R_S^2}{R_E} \int_{h \in \mathcal{H}_S} \frac{f_{H_S}(h)}{(h + R_S)} \cdot \left( \eta \left( \beta_S, m_S, \bar{G}_S P_S s, \sqrt{(R_S + h)^2 - R_E^2} \right) - \right. \right. \\ &\quad \left. \left. \eta \left( \beta_S, m_S, \bar{G}_S P_S s, \min(\max(r, R_S - R_E + h), \sqrt{(R_S + h)^2 - R_E^2}) \right) \right) dh \right), \end{aligned} \quad (73)$$

where  $\eta(\beta, m, s, x)$  is (44), obtained by the integration  $\int 1 - \frac{1}{(1+(sv^{-\beta})/m)^m} v dv = \eta(\beta, m, s, v)$ . The conditional Laplace transform of the terrestrial interference is derived in the equivalent manner. This completes the proof.

## APPENDIX E

### PROOF OF THEOREM 1

We recall that the rate coverage probability is expressed as

$$P^{\text{cov}}(\gamma, \lambda_o, \beta_o, m_o, f_{H_o}, R_S, R_E) \quad (74)$$

$$= \mathbb{P}[\mathcal{V}_S] \pi(S|\mathcal{V}_S) \mathbb{P}[R_{|S} > \gamma | \{o^* = S\}, \mathcal{V}_S] + \mathbb{P}[\mathcal{V}_T] \pi(T|\mathcal{V}_T) \mathbb{P}[R_{|T} > \gamma | \{o^* = T\}, \mathcal{V}_T]. \quad (75)$$

Conditioned on that the typical user is associated with the satellite network, the SINR is

$$\text{SINR}_{|S} = \frac{X_1^S \|\hat{\mathbf{d}}_1^S - \mathbf{u}_1\|^{-\beta_S}}{\tilde{I}_{S|S} + \tilde{I}_{T|S} + \tilde{\sigma}_{|S}^2}, \quad (76)$$

where  $\tilde{I}_{S|S} = \sum_{\mathbf{d}_i^S \in \tilde{\mathcal{B}}_{S|S}} \tilde{G}_{S/S} X_i^S \|\hat{\mathbf{d}}_i^S - \mathbf{u}_1\|^{-\beta_S}$ ,  $\tilde{I}_{T|S} = \sum_{\mathbf{d}_i^T \in \tilde{\mathcal{B}}_{T|S}} \tilde{G}_{T/S} \tilde{P}_{T/S} X_i^T \|\hat{\mathbf{d}}_i^T - \mathbf{u}_1\|^{-\beta_T}$ , and  $\tilde{\sigma}_{|S}^2 = \frac{\sigma^2}{G_S P_S}$ . We also have  $\tilde{G}_{S/S} = \bar{G}_S / G_S$ ,  $\tilde{G}_{T/S} = \bar{G}_T / G_S$ , and  $\tilde{P}_{T/S} = P_T / P_S$ . Since the conditional rate coverage probability is

$$\mathbb{P}[R_{|S} > \gamma | \{o^* = S\}, \mathcal{V}_S] = \mathbb{P}[\text{SINR}_{|S} > \tilde{\gamma}, | \{o^* = S\}, \mathcal{V}_S], \quad (77)$$

where  $\tilde{\gamma} = 2^{\gamma/W} - 1$ , the conditional probability (77) is derived as

$$\begin{aligned} \mathbb{P}[\text{SINR}_{|S} > \tilde{\gamma} | \{o^* = S\}, \mathcal{V}_S] &= \mathbb{E}[\mathbb{P}[\text{SINR}_{|S} > \tilde{\gamma} | \{o^* = S\}, \mathcal{V}_S, r]] \\ &\stackrel{(a)}{=} \mathbb{E}\left[\sum_{k=1}^{m_S-1} \frac{m_S^k r^{k\beta_S} \tilde{\gamma}^k}{k!} (-1)^k \frac{\partial^k \mathcal{L}_{I_{\text{tot}-S}}(s)}{\partial s^k} \Big|_{s=m_S \tilde{\gamma} r^{\beta_S}}\right], \end{aligned} \quad (78)$$

where (a) follows that  $\sqrt{X_1^S}$  follows the Nakagami- $m$  distribution with  $m_S$  and  $\mathcal{L}_{I_{\text{tot}-S}}(s) = \mathcal{L}_{I_S}\left(\frac{s}{G_S P_S} | r\right) \cdot \mathcal{L}_{I_T}\left(\frac{s}{G_S P_S} | \left(\frac{P_T B_T}{P_S B_S}\right)^{\frac{1}{\beta_T}} r^{\frac{\beta_S}{\beta_T}}\right) \cdot \exp(-s \tilde{\sigma}_{|S}^2)$ . We note that the expectation in (78) is associated with the conditional nearest satellite distance whose PDF is obtained in Lemma 4. Plugging (27) into (78), we get (48). Next, we obtain the rate coverage probability under the condition that the typical user is associated with the terrestrial network. Similar to the satellite network association case, we have

$$\text{SINR}_{|T} = \frac{X_1^T \|\hat{\mathbf{d}}_1^T - \mathbf{u}_1\|^{-\beta_T}}{\tilde{I}_{S|T} + \tilde{I}_{T|T} + \tilde{\sigma}_{|T}^2}, \quad (79)$$

where  $\tilde{I}_{S|T} = \sum_{\mathbf{d}_i^S \in \tilde{\mathcal{B}}_{S|T}} \tilde{G}_{S/T} \tilde{P}_{S/T} X_i^S \|\hat{\mathbf{d}}_i^S - \mathbf{u}_1\|^{-\beta_S}$ ,  $\tilde{I}_{T|T} = \sum_{\mathbf{d}_i^T \in \tilde{\mathcal{B}}_{T|S}} \tilde{G}_{T/T} X_i^T \|\hat{\mathbf{d}}_i^T - \mathbf{u}_1\|^{-\beta_T}$ , and  $\tilde{\sigma}_{|T}^2 = \frac{\sigma^2}{G_T P_T}$ , with  $\tilde{G}_{S/T} = \bar{G}_S / G_T$ ,  $\tilde{G}_{T/T} = \bar{G}_T / G_T$ , and  $\tilde{P}_{S/T} = P_S / P_T$ . The rate

coverage probability for the terrestrial network association case is  $\mathbb{P}[R_{|\text{T}} > \gamma | \{o^* = \text{T}\}, \mathcal{V}_{\text{T}}] = \mathbb{E}[\mathbb{P}[\text{SINR}_{|\text{T}} > \tilde{\gamma}, |\{o^* = \text{T}\}, \mathcal{V}_{\text{T}}, r]]$ , which gives

$$\mathbb{E}[\mathbb{P}[\text{SINR}_{|\text{T}} > \tilde{\gamma}, |\{o^* = \text{T}\}, \mathcal{V}_{\text{T}}, r]] = \mathbb{E}\left[\sum_{k=1}^{m_{\text{T}}-1} \frac{m_{\text{T}}^k r^{k\beta_{\text{T}}} \tilde{\gamma}^k}{k!} (-1)^k \cdot \frac{\partial^k \mathcal{L}_{I_{\text{tot-T}}}(s)}{\partial s^k} \Big|_{s=m_{\text{T}} \tilde{\gamma} r^{\beta_{\text{T}}}}\right], \quad (80)$$

where  $\mathcal{L}_{I_{\text{tot-T}}}(s) = \mathcal{L}_{I_{\text{S}}}\left(\frac{s}{G_{\text{T}}P_{\text{T}}} \mid \left(\frac{P_{\text{S}}B_{\text{S}}}{P_{\text{T}}B_{\text{T}}}\right)^{\frac{1}{\beta_{\text{S}}}} r^{\frac{\beta_{\text{T}}}{\beta_{\text{S}}}}\right) \cdot \mathcal{L}_{I_{\text{T}}}\left(\frac{s}{G_{\text{T}}P_{\text{T}}} \mid r\right) \exp\left(-s\tilde{\sigma}_{|\text{T}}^2\right)$ . Since the expectation in (80) is associated with the conditional nearest terrestrial BS's distance whose PDF is obtained in Corollary 3. Eventually, we reach (49). This completes the proof.

## REFERENCES

- [1] J. C. McDowell, "The low earth orbit satellite population and impacts of the SpaceX Starlink constellation," *The Astrophysical Journal Letters*, vol. 892, no. 2, p. L36, apr 2020.
- [2] J. P. Choi and C. Joo, "Challenges for efficient and seamless space-terrestrial heterogeneous networks," *IEEE Commun. Mag.*, vol. 53, no. 5, pp. 156–162, 2015.
- [3] H. Yao, L. Wang, X. Wang, Z. Lu, and Y. Liu, "The space-terrestrial integrated network: An overview," *IEEE Commun. Mag.*, vol. 56, no. 9, pp. 178–185, 2018.
- [4] P. Wang, J. Zhang, X. Zhang, Z. Yan, B. G. Evans, and W. Wang, "Convergence of satellite and terrestrial networks: A comprehensive survey," *IEEE Access*, vol. 8, pp. 5550–5588, 2020.
- [5] B. Di, H. Zhang, L. Song, Y. Li, and G. Y. Li, "Ultra-dense LEO: Integrating terrestrial-satellite networks into 5g and beyond for data offloading," *IEEE Trans. Wireless Commun.*, vol. 18, no. 1, pp. 47–62, 2019.
- [6] W. Abderrahim, O. Amin, M.-S. Alouini, and B. Shihada, "Proactive traffic offloading in dynamic integrated multisatellite terrestrial networks," *IEEE Trans. Commun.*, vol. 70, no. 7, pp. 4671–4686, 2022.
- [7] D. Wang, W. Wang, Y. Kang, and Z. Han, "Distributed data offloading in ultra-dense LEO satellite networks: A Stackelberg mean-field game approach," *IEEE J. Sel. Topics Signal Process.*, vol. 17, no. 1, pp. 112–127, 2023.
- [8] F. Baccelli and B. Błaszczyszyn, "Stochastic geometry and wireless networks: Volume i theory," *Found. Trends in Networking*, vol. 3, no. 3–4, p. 249–449, Mar. 2009.
- [9] M. Haenggi, J. G. Andrews, F. Baccelli, O. Dousse, and M. Franceschetti, "Stochastic geometry and random graphs for the analysis and design of wireless networks," *IEEE J. Sel. Areas Commun.*, vol. 27, no. 7, pp. 1029–1046, 2009.
- [10] S. Singh, H. S. Dhillon, and J. G. Andrews, "Offloading in heterogeneous networks: Modeling, analysis, and design insights," *IEEE Trans. Wireless Commun.*, vol. 12, no. 5, pp. 2484–2497, 2013.
- [11] S. Singh and J. G. Andrews, "Joint resource partitioning and offloading in heterogeneous cellular networks," *IEEE Trans. Wireless Commun.*, vol. 13, no. 2, pp. 888–901, 2014.
- [12] J. Park, N. Lee, J. G. Andrews, and R. W. Heath, "On the optimal feedback rate in interference-limited multi-antenna cellular systems," *IEEE Trans. Wireless Commun.*, vol. 15, no. 8, pp. 5748–5762, 2016.
- [13] N. Lee, D. Morales-Jimenez, A. Lozano, and R. W. Heath, "Spectral efficiency of dynamic coordinated beamforming: A stochastic geometry approach," *IEEE Trans. Wireless Commun.*, vol. 14, no. 1, pp. 230–241, 2015.
- [14] T. Bai, A. Alkhatieb, and R. W. Heath, "Coverage and capacity of millimeter-wave cellular networks," *IEEE Commun. Mag.*, vol. 52, no. 9, pp. 70–77, 2014.

- [15] J. Park, J. G. Andrews, and R. W. Heath, "Inter-operator base station coordination in spectrum-shared millimeter wave cellular networks," *IEEE Trans. Cognitive Commun. and Networking*, vol. 4, no. 3, pp. 513–528, 2018.
- [16] V. V. Chetlur and H. S. Dhillon, "Downlink coverage analysis for a finite 3-D wireless network of unmanned aerial vehicles," *IEEE Trans. Commun.*, vol. 65, no. 10, pp. 4543–4558, 2017.
- [17] M. Banagar and H. S. Dhillon, "Performance characterization of canonical mobility models in drone cellular networks," *IEEE Trans. Wireless Commun.*, vol. 19, no. 7, pp. 4994–5009, 2020.
- [18] A. Al-Hourani, "An analytic approach for modeling the coverage performance of dense satellite networks," *IEEE Wireless Commun. Lett.*, vol. 10, no. 4, pp. 897–901, 2021.
- [19] —, "Optimal satellite constellation altitude for maximal coverage," *IEEE Wireless Commun. Lett.*, vol. 10, no. 7, pp. 1444–1448, 2021.
- [20] N. Okati, T. Riihonen, D. Korpi, I. Angervuori, and R. Wichman, "Downlink coverage and rate analysis of low Earth orbit satellite constellations using stochastic geometry," *IEEE Trans. Commun.*, vol. 68, no. 8, pp. 5120–5134, 2020.
- [21] N. Okati and T. Riihonen, "Nonhomogeneous stochastic geometry analysis of massive LEO communication constellations," *IEEE Trans. Commun.*, vol. 70, no. 3, pp. 1848–1860, 2022.
- [22] D.-H. Jung, J.-G. Ryu, W.-J. Byun, and J. Choi, "Performance analysis of satellite communication system under the shadowed-Rician fading: A stochastic geometry approach," *IEEE Trans. Commun.*, vol. 70, no. 4, pp. 2707–2721, 2022.
- [23] D.-H. Na, K.-H. Park, Y.-C. Ko, and M.-S. Alouini, "Performance analysis of satellite communication systems with randomly located ground users," *IEEE Trans. Wireless Commun.*, vol. 21, no. 1, pp. 621–634, 2022.
- [24] J. Park, J. Choi, and N. Lee, "A tractable approach to coverage analysis in downlink satellite networks," *IEEE Trans. Wireless Commun.*, pp. 1–1, 2022.
- [25] Z. Song, J. An, G. Pan, S. Wang, H. Zhang, Y. Chen, and M.-S. Alouini, "Cooperative satellite-aerial-terrestrial systems: A stochastic geometry model," *IEEE Trans. Wireless Commun.*, vol. 22, no. 1, pp. 220–236, 2023.
- [26] B. A. Homssi and A. Al-Hourani, "Modeling uplink coverage performance in hybrid satellite-terrestrial networks," *IEEE Commun. Lett.*, vol. 25, no. 10, pp. 3239–3243, 2021.
- [27] H. Cundy and A. Rollett, "Sphere and cylinder—Archimedes' theorem," *Mathematical Models*, pp. 172–173, 1989.
- [28] G. Giunta, C. Hao, and D. Orlando, "Estimation of Rician K-factor in the presence of nakagami- $m$  shadowing for the LoS component," *IEEE Wireless Commun. Lett.*, vol. 7, no. 4, pp. 550–553, 2018.
- [29] M. Di Renzo, "Stochastic geometry modeling and analysis of multi-tier millimeter wave cellular networks," *IEEE Trans. Wireless Commun.*, vol. 14, no. 9, pp. 5038–5057, 2015.
- [30] J. G. Andrews, F. Baccelli, and R. K. Ganti, "A tractable approach to coverage and rate in cellular networks," *IEEE Trans. Commun.*, vol. 59, no. 11, pp. 3122–3134, 2011.
- [31] H. Alzer, "On some inequalities for the incomplete Gamma function," *Mathematics of Computation*, vol. 66, no. 218, pp. 771–778, 1997.
- [32] A. K. Gupta, J. G. Andrews, and R. W. Heath, "On the feasibility of sharing spectrum licenses in mmWave cellular systems," *IEEE Trans. Commun.*, vol. 64, no. 9, pp. 3981–3995, 2016.
- [33] Y. Li, J. G. Andrews, F. Baccelli, T. D. Novlan, and C. J. Zhang, "Design and analysis of initial access in millimeter wave cellular networks," *IEEE Trans. Wireless Commun.*, vol. 16, no. 10, pp. 6409–6425, 2017.
- [34] H. Elshaer, M. N. Kulkarni, F. Boccardi, J. G. Andrews, and M. Dohler, "Downlink and uplink cell association with traditional macrocells and millimeter wave small cells," *IEEE Trans. Wireless Commun.*, vol. 15, no. 9, pp. 6244–6258, 2016.
- [35] J.-S. Ferenc and Z. Néda, "On the size distribution of Poisson Voronoi cells," *Physica A: Statistical Mechanics and its Applications*, vol. 385, no. 2, pp. 518–526, 2007.